ORIGINAL ARTICLE
DOI: https://doi.org/10.30932/1992-3252-2023-21-3-1

World of Transport and Transportation, 2023,
Vol. 21, Iss. 3 (106), pp. 154–182

Geophysical Processes in the Arctic and the System Analysis of their Impact on Operation and Development of the Transport Infrastructure

Alexey D. GVISHIANI

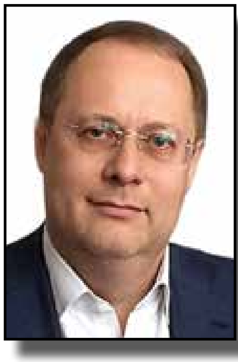

Igor N. ROZENBERG

Anatoly A. SOLOVIEV

Alexey D. Gvishiani [1], ***Igor N. Rozenberg*** [2], ***Anatoly A. Soloviev*** [3]

[1, 3] *Geophysical Centre of the Russian Academy of Sciences, Moscow, Russia.*
[2] *Russian University of Transport, Moscow, Russia.*
[1, 3] *Schmidt Institute of Physics of the Earth of the Russian Academy of Sciences, Moscow, Russia.*
[2] *JSC NIIAS, Moscow, Russia.*
✉ *i.rozenberg@geosc.ru.*

ABSTRACT

The scientific research that has become the subject of consideration in this article is related to assessment of the influence of geophysical factors on sustainable functioning of transport systems and the system analysis of their impact on the transport infrastructure at the Arctic latitudes. The research is a new direction in the field of study of operational reliability of transport systems and scientific support for development of transport infrastructure in the Russian Arctic.

The paper touches upon the issues of reliability and possible failures of technical equipment under the influence of space weather, and also discusses multifaceted problems of safety and efficiency of development of transport systems considering new data on the structure and properties of the lithosphere referring to thawing of permafrost and mineral deposits. A separate section is devoted to new information on seismic activity and seismic hazard assessment in areas of operation and promising development of the transport infrastructure of the Arctic zone of the Russian Federation (AZRF).

Intellectual accounting and generalisation of the obtained interdisciplinary results together with their visualisation are provided by geoinformatics methods. The paper presents also the results of adoption of modern geodatabase management systems, of the application of modern technologies of geoportals and interactive spherical visualisations for qualitative presentation of new geophysical knowledge obtained in the course of research.

Keywords: *geomagnetism, seismic hazard, geophysical processes, geological structures, geoinformatics, Arctic zone of the Russian Federation, transport systems, transport infrastructure, sustainable development.*

Funding: *The work was supported by the Russian Science Foundation Grant No. 21–77–30010 «System Analysis of the Dynamics of Geophysical Processes in the Russian Arctic and Their Impact on Development and Operation of the Railway Transport Infrastructure».*

For citation: *Gvishiani, A. D., Rozenberg, I. N., Soloviev, A. A. Geophysical Processes in the Arctic and the System Analysis of their Impact on Operation and Development of the Transport Infrastructure. World of Transport and Transportation, 2023, Vol. 21, Iss. 3 (106), pp. 154–182. DOI: https://doi.org/10.30932/1992-3252-2023-21-3-1.*

The text of the article originally written in Russian is published in the first part of the issue.
Текст статьи на русском языке публикуется в первой части данного выпуска.

INTRODUCTION

The active development of the Russian Arctic in the 21st century is inevitably associated with widespread involvement of high technologies. Such technologies, first, are necessary for stable development of industry and transport in hard-to-reach regions and under extreme climatic conditions inherent in the Arctic region. However, being resilient to these natural factors, complex technological systems often become sensitive to other natural risks.

For example, extended power lines (PL) and pipelines in high-latitude areas effectively cope with low temperatures, confidently performing their functions over vast areas. At the same time, their sustainable functioning is threatened by extreme manifestations of space weather. The latter can lead to excessive loads on electric power systems and installations that provide anti-corrosion protection of pipelines, up to their complete failure. Thus, besides climate change [1], a number of purely geological and geophysical factors should be taken into account both for sustainable operation of existing high-tech systems in the Arctic, and when planning further development of these infrastructures in still insufficiently developed regions.

The modern technological society is a complex interweaving of dependencies and interdependencies between several of its critical infrastructures [2]. As technological infrastructures become more complex, any major disruption to one of them can have wide-ranging consequences for others and lead to interdependent failures [3]. The impact on these interdependent infrastructures can last for several years with a probability of manifestation of significant social and economic impacts [4; 5].

The development of transport infrastructure is of critical importance for both partial and full-scale development of the Arctic zone of the Russian Federation (AZRF). This is also emphasised by the «Strategy for development of the Arctic zone of the Russian Federation and ensuring national security for the period until 2035», approved by Decree of the President of the Russian Federation of October 26, 2020, No. 645. Besides other points, this strategy provides for a significant development of transport infrastructure in a number of northern regions of Russia, which includes construction of new railways, interregional roads and airports, creation of waterways, taking into account plans for development of the mineral resource base and ensuring the connectivity of seaports with the country's inland territories. The integrated, interconnected, and systemic development of the infrastructure of maritime, air, rail and road transport in the Russian Arctic implies an intensive build-up of systematic fundamental and applied research in the interests of studying and developing the Arctic, considering the extreme natural and climatic features of the region. Scientific support for development of transport systems involves a system-analytical consolidation of the efforts of experts of various geophysical and related areas, such as geomagnetism [6; 7], seismology, climatology, geotectonics, geoinformatics, etc. Effective intellectual accounting and generalisation of the obtained interdisciplinary results are provided through system analysis.

In this paper, the authors intend to focus on several important geological and geophysical results. Each of them individually and all of them on the whole are of critical importance and require undoubted consideration for the purposes of operation and development of transport infrastructure in the Russian Arctic. The first section presents the results of assessment of the negative impact of space weather on operation of modern railway signalling electronics, power supply, and positioning and navigation accuracy. The second section presents new results on the study of large geological structures and sedimentary basins. The latter may be associated with hydrocarbon deposits, as well as other important geophysical characteristics of the Arctic lithosphere. The third section provides new important information about the seismic activity of the Russian Arctic. The fourth section contains the results in the field of geoinformatics, obtained by integrating new data in a single environment in three listed areas. This opens up the possibility of complex processing, system analysis and visualisation of the obtained geophysical results. The conclusions are presented in the final section of the article.

Scientific research, which has become the subject of this article, is a new direction in the field of operational reliability of transport systems. The most pressing issues for transport – reliability and safety, have been repeatedly considered in various aspects in many publications of the *World of Transport and Transportation* journal. But the influence of geophysical factors on sustainable functioning of transport systems, a systematic analysis of their impact on the transport infrastructure in the Arctic are presented for the first time.

RESULTS

1. Influence of space weather on functioning of transport and auxiliary engineering systems at the high latitudes of the Russian Federation

1.1. The impact of geomagnetic activity on failures in operation of railway signal automation

Space weather is mainly determined by solar flares, coronal mass ejections, high-speed plasma flows from solar holes that cause geomagnetic storms and substorms. The total amount of energy released during a medium-intensity magnetic storm is about 1400 GW, which is almost twice the capacity of all US power plants. Long-distance infrastructure networks, such as railways located at high latitudes, are affected by geomagnetic disturbances [8; 9]. During geomagnetic storms, the Earth's magnetic field can change rapidly and strongly over time, which provokes the appearance of an electric potential difference of up to several volts per kilometer, which in turn leads to the appearance of geomagnetically induced currents (GIC) in extended conductors. GIC can have a significant impact on operation of engineering systems. From a railway safety point of view, the most important systems that can be affected by GIC are signalling and traffic control systems [10]. During strong geomagnetic disturbances, cases of short-term (1–2 minutes) false occupancy of tracks are observed, which can be repeated for 3–4 hours [11]. The occurrence of signal anomalies is explained by induced currents in the earth during strong geomagnetic storms. Under these conditions, the natural electric field is strong enough to reduce the operating voltage across the relay. Depending on the direction of the GIC in the rails, both a false red light can light up when the track is free (any direction of GIC), and a false green light can light up when it is occupied (GIC with the opposite sign). Of course, the false green light is the most dangerous.

Historically, the first reported event associated with a railway signalling failure was the New York Railroad Storm on May 13, 1921 [12]. A storm of exceptional strength occurred in the fourth year after the maximum of the 15th solar cycle [13]. The prelude of this magnetic storm was a double flash on the limb of the Sun, visible even to the naked eye [14]. As an example of modern incidents, let's take a storm in July 1982, when failures in operation of railway automation were noted in southern Sweden [15]. The magnetic storm of July 13–14, 1982 developed against the background of a decline in the solar cycle and reached a maximum of Dst = –325 nT. During development of the disturbance on the Swedish Railways, there were problems with light signalling: the signal traffic light switched between red and green light for no apparent reason.

In Russia, studies of the relationship between anomalies in operation of railway signalling and geomagnetic disturbances began relatively recently [16]. So, in [10; 17; 18] the statistical relationship between the level of geomagnetic activity and duration of failures in operation of automation systems of the East Siberian Railway in 2004 were studied. It was shown that the total daily duration of anomalies not associated with mechanical damage and meteorological causes on all sections of the road varies in accordance with development of a geomagnetic storm. This duration increases three times when the peak of geomagnetic activity is reached and correlates with the local index of geomagnetic activity. Thus, during strong storms, an increase in the number of disruptions is observed even at middle latitudes.

When analysing failures in operation of signalling systems on the Northern Railway [11], it was revealed that almost every strong geomagnetic storm out of 16 analysed was the cause of anomalies in operation of signal automation. The distribution of registered anomalies per local time slots obtained in the work is consistent with known distributions of the periods of GIC development [19; 20]. Failures in operation of automation systems, in particular, false alarms of traffic lights, were associated with induction of an electric field on rails across the track, which could cause an imitation of a passed locomotive. Analysing failures in operation of the signal automation of the Northern and Oktyabrskaya Railways for 2009–2010 (the 23rd cycle of solar activity), the authors of [21] found that anomalies in operation of automation systems develop almost synchronously and in close connection with excitation of significant geoelectric fields.

To clarify the regularities in manifestation of the impact of geomagnetic disturbances on operation of railway automation and to find ways to limit the impact, it seems appropriate to study

Pic. 1. The considered section of Oktyabrskaya railway (yellow dotted line) and the location of Lovozero magnetic station (IAGA code LOZ, red) in Murmansk region [prepared with participation of the authors].

in detail anomalies in operation of automation and signalling systems in sections of railway networks located primarily in the Arctic and subarctic zones. In this regard, an extensive archive of log records of logged failures in operation of railway automation was analysed at the section of Oktyabrskaya railway from the station Kandalaksha (67.15° N) to the station Nickel-Murmansky (69.4° N) for 2001–2006 (Pic. 1). The archive contained information on more than 1800 records, and such a volume of information about failures was analysed for the first time [22].

In the archive, for some events, the reason was indicated, for some – not. The reasons indicated in the reports and records of the railway services, as a rule, were associated with breaks, shocks, and mechanical breaks in cables, with meteorological reasons (ice and sand getting into the turnout switches), with intervention of unauthorised persons, that is, they were obviously not caused by geomagnetic factors. For a thorough statistical analysis, the entire archive was divided into the following three categories of events:

1. Periods without failures lasting more than 1 day.
2. Failures without an obvious external cause.
3. Failures with an indication of the cause (most often mechanical damage, meteorological reasons or interference by unauthorised persons).

It was a priori assumed that failures with no apparent external cause (Category 2) were more likely to be caused by space weather disturbances. Interruption periods were compared with different types of geomagnetic disturbances using four independent statistical tests based on different principles. Geomagnetic disturbances were estimated using the geomagnetic indices of auroral activity AE and interplanetary magnetic cloudiness EI, as well as the spectral density of Pc5 type geomagnetic pulsations recorded at the nearby Lovozero magnetic observatory (IAGA code LOZ, Murmansk region, Pic. 1). The analysis showed that the probability of occurrence of failures increases with the level of geomagnetic

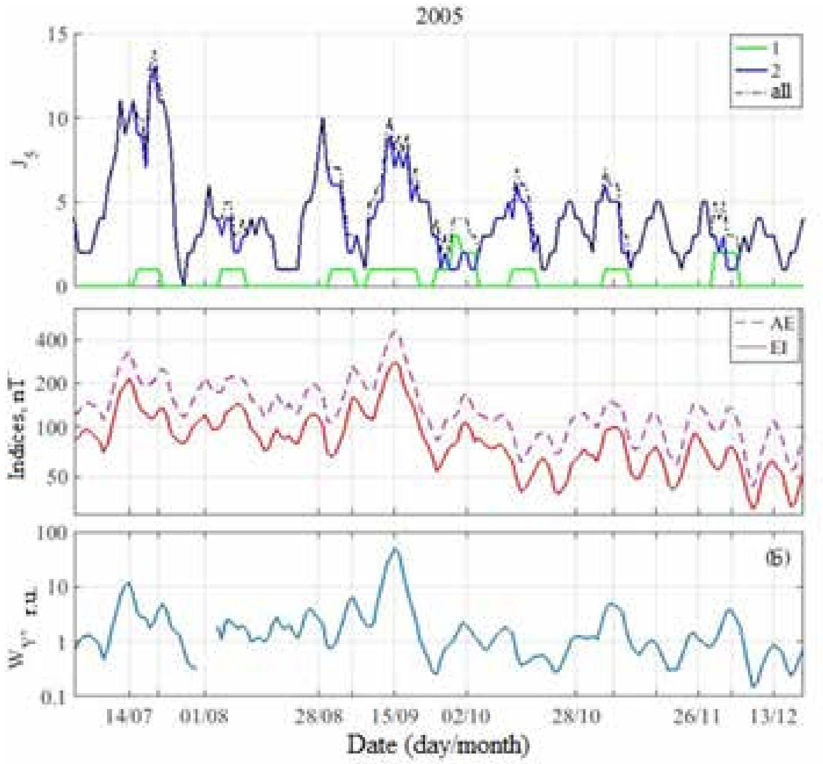

Pic. 2. Frequency of failures of category 1, 2 and events of all three categories (upper graph), AE and EI geomagnetic indices (middle graph), and spectral density of Pc5-type geomagnetic pulsations recorded at LOZ magnetic station for the period July-December 2005 [prepared with participation of the authors].

activity. At the same time, integral values of geomagnetic indices over 2–4 days turn out to be significant, which corresponds to the average duration of geomagnetic storms. Another important result was that category 3 failures, the cause of which was clearly indicated in the archive, do not show differences in the statistical relationship with geomagnetic activity. Possible explanations for this can be both technical factors associated with inaccuracies in the description of the causes, and physical factors associated with the indirect influence of geomagnetic activity through the weather. Pic. 2 shows graphs of variability of geomagnetic activity and the frequency of failures of railway signal automation for July-December 2005. The graph clearly shows the coincidence of all maxima of auroral activity and local geomagnetic disturbance with the maxima of frequency of anomalous events.

The analysis of the GIC amplitude (e. g., [23; 24]) and failures on the railway shows that the source of the strongest disturbances is the auroral oval, namely, the region of discrete precipitation, which gravitates closer to the equatorial boundary of the oval. It is important to note that the stronger is the geomagnetic disturbance, the lower are the latitudes to which the auroral zone shifts. Thus, the critical problem is the possibility of predicting the position of the oval and auroral precipitation. In this regard, an online service for short-term forecasting of intensity and spatial distribution of auroras was developed (Pic. 3). The input parameters are real-time data from interplanetary satellites located at L1 libration point, which provides a forecast with a horizon of 30–70 min. The developed system is based on the empirical mathematical model OVATION-Prime [25], which establishes statistical relationships between the parameters of the solar wind, the interplanetary magnetic field, and auroral particle fluxes. It has been shown that the proportion of confirmed aurora forecasts is more than 86 % [26; 27].

1.2. Exposure of global satellite navigation systems in the auroral region to geomagnetic activity

Transport relies heavily on availability of other critical infrastructures such as power, signalling, communications and navigation

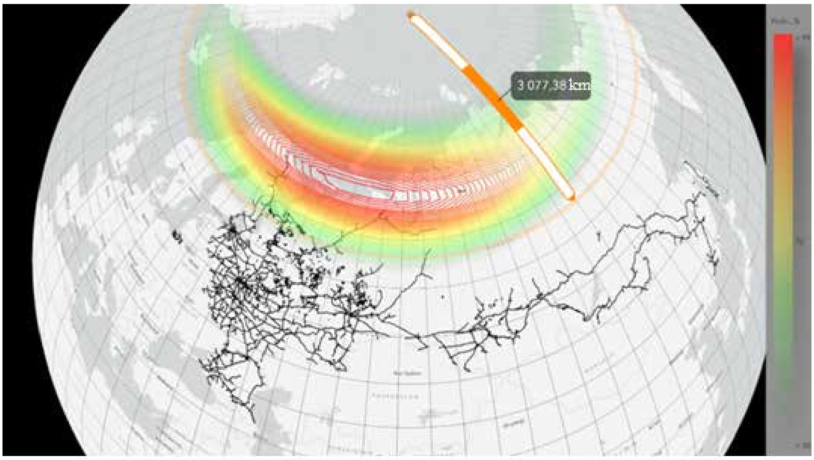

Pic. 3. An example of modelling the position of the auroral oval and the intensity of auroras online (http://aurora-forecast.ru).

systems for operations and positioning, and previous research has shown that these technologies can be disrupted during space weather. Due to introduction of digital technologies in railways, such as big data [28], service 4.0 [29], the Internet of things (IoT) [30], cyber-physical systems [31], there may also be failures in operation of other digital electronic equipment [32]. Thus, technological advances have increased the risk of adverse effects caused by a solar storm. Let us dwell in more detail on the impact of space weather on satellite navigation systems.

Global navigation satellite systems (GNSS) use signal transmission in the range from units to tens of GHz from a magnetospheric satellite. The region of the magnetosphere where the maximum number of navigation satellites is concentrated includes the geostationary orbit (distance to the center of the Earth 6,6R_E, where R_E is the radius of the Earth) and lower orbits. The satellite electronics itself is exposed to fast charged particles, primarily the electrons of radiation belts, and can be damaged during sharp increases in electron fluxes. But the number of navigation satellites is currently so high that damage or even loss of one of the satellites can only slightly affect the quality of navigation in most areas. Nevertheless, the question of the increase in the error associated with a decrease in the number of satellites for a particular receiving point requires a separate study, as well as modelling the loss of a signal from several satellites simultaneously under conditions of extreme increases in the electron flux. Modern navigation systems are based on the use of several systems, including GNSS: GPS (USA), GLONASS (Russian Federation), Galileo (European Union), BeiDou/Compass (PRC).

In the autonomous navigation mode, the positioning error is a few meters. Let us consider the physical mechanisms of the influence of space weather disturbances on accuracy of the navigation signal reception. With all the variety of effects, they fit into the following main groups:

1. Deterioration of the signal-to-noise ratio due to natural noise in the operating range of the emitter.

2. Damage to the transmitting equipment by streams of fast charged particles.

3. Disturbances on the propagation path from the transmitter to the receiver, primarily due to ionospheric inhomogeneities.

The source of the first group of distortions is the increase in the flux of solar radio emission during flares. Damage to equipment on magnetospheric satellites whose orbit lies inside the Earth's magnetosphere is associated with increases in fluxes of fast charged particles of both solar and magnetospheric origin. The maximum amplitudes of ionospheric inhomogeneities are associated with the zone of auroras and, above all, their discrete forms.

Thus, possible cosmic sources of errors in operation of navigation equipment are associated with solar flares, solar proton, and electron events, increases in fast electron fluxes in the magnetosphere, and powerful auroral disturbances. The effects associated with charged particles and ionospheric inhomogeneities are most pronounced during strong magnetic storms, when not only the disturbance amplitudes increase, but the disturbance maximum shifts to the mid-latitude region [33].

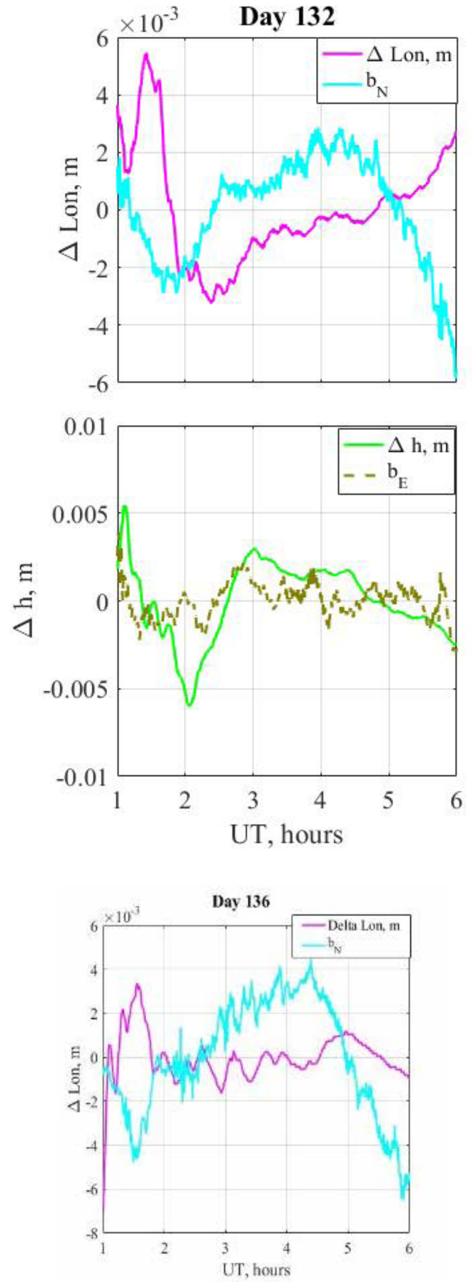

Pic. 4. Examples of consistent positioning error variations in longitude (top) and altitude (bottom) at SVTL base station (60.5o N, 29o E, Leningrad region) and magnetic field variations at NUR station (60.5o N, 25.5o E, Finland) during the time of the main (left) and recovery (right) phases of the magnetic storm on May 12, 2021. The amplitude of the magnetic field variations is normalised by the amplitude of the displacement variations [performed by the authors].

The sun is a source of electromagnetic radiation in a wide range of wavelengths, including the frequency range of GNSS signals (1–2 GHz). This leads to a deterioration in the signal-to-noise ratio when receiving a signal from the satellite. Statistical analysis of the effect of solar flares on the signal-to-noise ratio showed that receivers operating at L2/L5 frequencies are the most vulnerable, and the signal quality at L1 frequency changes little [34]. At the same time, an increase in the number of satellites for this type of interference does not lead to a significant improvement in the situation, since an increase in noise associated with a flare affects all visible satellites simultaneously [35]. A significant improvement in the signal-to-noise ratio occurred due to an increase in the power of the useful signal on new generations of satellites, which makes it possible to maintain operability for flares with a radio flux exceeding 20000 units, which are observed from 1 to several times a year, depending on the phase of the solar cycle [34]. A comparative analysis of the effect of flares in 2011 and 2017, performed in [36], showed a significant weakening of the effect of solar radio flares for new, more powerful systems.

To test the hypothesis of the effect of geomagnetic activity on geopositioning accuracy, we used data from GNSS base stations in auroral and subauroral latitudes. The time resolution was 30 s. Standard primary processing made it possible to compensate for most of ionospheric disturbances. For base stations, the number of satellites in all cases was 15 or more. To test the impact on accuracy of geopositioning, 4 groups of days were selected according to the types of geomagnetic disturbances, for which the following codes were used:

1. lack of disturbance.
2. geomagnetic storms.
3. auroral substorms of high intensity.
4. solar radio flares.

To control the low magnetic activity (code 0), we considered days satisfying the following conditions: the absence of solar radio flares, the absence of magnetic storms with Dst<–50 nT and missing the 4-day window before the storm, and the absence of auroral disturbances with AE>100 nT. For each disturbance, the most probable geographic zone (minimum and maximum latitudes and longitudes) of the maximum effect was determined by its type and onset time. In total, 38 events with code 0, 10 events with code 1, 38 events with code 2, and 5 events with code 3 were selected for 2020–2023.

The analysis of the effect of space weather disturbances on time scales from several minutes to several hours showed that even for a base station, after applying the differential correction algorithm [37], in the apparent longitudinal and

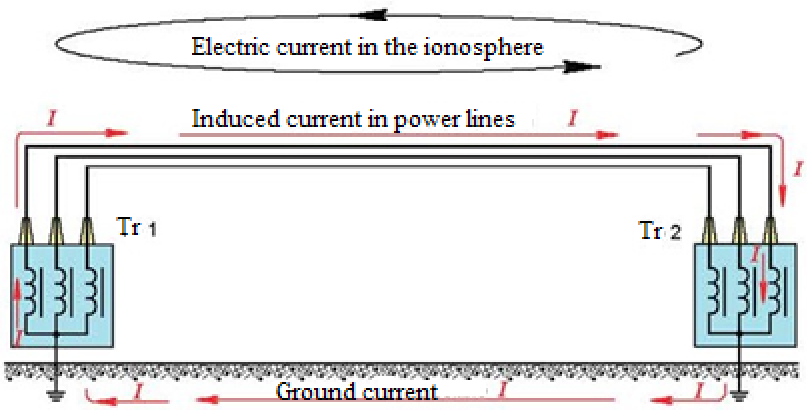

Pic. 5. Scheme of formation and flow of GIC in power lines [compiled with participation of the authors].

vertical displacements determined from the GNSS, variations remain in the range of periods of 5–20 minutes, coinciding in frequencies with geomagnetic field variations at the nearest magnetometric station. The amplitudes of these variations for base stations vary within a few centimeters (Pic. 4).

To use the results of signal analysis at the base station in real applications, it is necessary to solve the following tasks:

1. Consideration of the difference between the actual number of satellites in place and at the base station.

2. Obtaining data with a higher temporal resolution to assess the possibility of applying them to a moving object (for example, rolling stock).

3. Exclusion of the differential correction method used in standard data preprocessing in the GNSS network, since it is aimed at geodesy problems and maximally suppresses variations within a day, which gives inconsistent results on different time scales (between days 0.1–10 m, within a day $<10^{-2}$ m).

1.3. Impact of space weather on electricity supply

Variations of geoelectric currents induced in the surface layers of the earth's crust are closed through grounded energy systems, causing the appearance of GIC [38; 39] (Pic. 5). In turn, GIC leads to voltage drops, overheating of power transformers and loss of reactive power in high-voltage power lines [40]. Currently, GIC have become a constant threat to high-tech societies and pose a serious threat to regional high-voltage electrical networks, many of which cross national borders [41]. In order to transmit large amounts of energy over long distances, more and more extended power lines are being built. However, such lines are particularly susceptible to large GIC. This circumstance makes electrical networks more and more susceptible to space weather disturbances.

The dependence of the railway sector on the electricity grid represents a critical vulnerability due to its direct impact on the railway network, but a power outage can also affect other systems in the station. Other railway equipment that may also be susceptible to GIC are roadside cables, telecommunications and line circuits, standby systems, batteries, condition monitoring systems, point circuits in switching [42].

When studying the excitation of GIC in real high-voltage lines, an important factor is continuous recording of excited currents in operating networks. In Russia, there is a system of continuous registration of GIC in the main line «Northern Transit», passing from the middle latitudes to the Arctic zone. The system has been operating for ten years, and the obtained data on development of GIC at various levels of geomagnetic disturbances make it possible to estimate the possible values of GIC during extreme disturbances. The maximum GIC values in the transformer neutral reached 140 A at the northernmost substation Vykhodnoy during the event on June 29, 2013. The extremely large value of current was determined by the nature of the disturbance, the train of Ps6 type pulsations during development of a strong substorm [43], and the configuration of connection of power

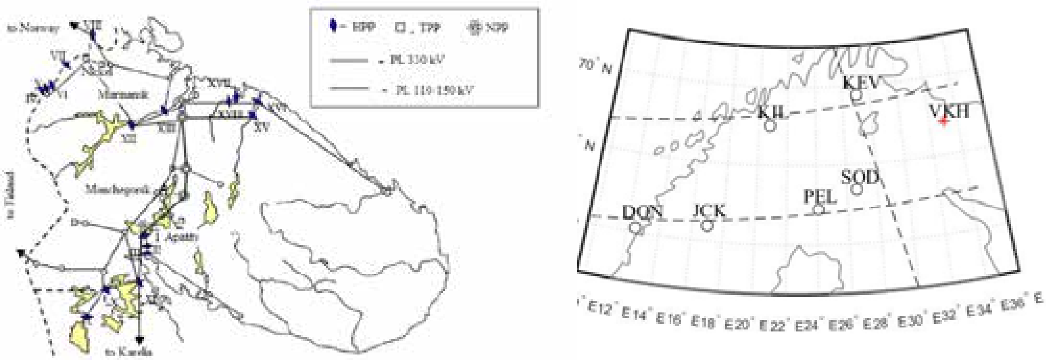

(a) (b)

Pic. 6. Scheme of the Northern Transit power line on the Kola Peninsula: (a) location of its northern substation Vykhodnoy (VKH), where GIC measurements are carried out; (b) location of nearby geomagnetic stations on the territory of Russia and Finland [compiled with participation of the authors].

equipment at the substation during the indicated period. With development of significant GIC in the neutral of the transformer, quality of electricity deteriorates significantly due to generation of harmonics of the fundamental frequency. It is the harmonics that can cause disturbances in the thermal regime of the transformer, disrupt operation of protective relays, and interfere with operation of equipment in networks of electricity consumers. To influence operation of the transformer, it is sufficient to excite GIC with an intensity of only a few A.

The calculation of possible GIC levels during typical and extreme magnetic storms, which can be used by network operators to take the necessary measures to reduce the risk of catastrophic consequences, is an extremely urgent task. Solving the problems of reducing the risk of occurrence and reducing the consequences of natural disasters does not come down simply to the «engineering» application of the results of space physics for calculating GIC in technological systems, but also requires elucidation of the physical nature of some magnetospheric-ionospheric phenomena. An effective prediction of GIC intensity and spatial distribution requires a thorough study of various types of trigger disturbances in the geomagnetic field. Magnetic storms are the most studied source of GIC. We conducted a study of GIC generated outside the storm, which showed that the most effective triggers are such auroral disturbances as isolated substorms and geomagnetic pulsations. To do this, we analysed simultaneously the data of the GIC registration system in the neutral of the transformer on the Northern Transit power line (Kola Peninsula, Republic of Karelia) (Pic. 6 (a)) and geomagnetic measurements obtained at nearby geomagnetic stations in Russia and Finland (Pic. 6 (b)), for 2014–2018.

As a result of the research, the following factors were identified that affect the GIC-efficiency of pulsations:

1. Spatial scale.
2. Shape of the spectrum.
3. Polarisation.

The analysis of data from several geomagnetic stations makes it possible to study spatial distribution of the pulsation field. It was shown that the same amplitude and frequency of perturbations can lead to different effects due to different spatial scales of pulsations [44]. The effect of spatial scale on GIC efficiency is clearly illustrated in Pic. 7. It can be seen from the picture that the ratio of GIC amplitude to the pulsation amplitude increases with an increase in the spatial scale of the pulsation field, which preserves the amplitude and frequency.

It was also shown that the spectral composition of ULF pulsations is a significant efficiency factor in generation of GIC [45]. In this regard, multiharmonic pulsations turn out to be more efficient than single-harmonic ones – in case of the former, the ratio of the GIC amplitude to the pulsation amplitude is one and a half times greater. Pic. 8 shows the spectra of the eastern *Y*-component of the pulsations and its time derivative at the top right. The shape of both spectra has a pronounced leading edge, which ensures the efficiency of GIC generation. In this case, the spectrum of the generated geoinduced current (the graph on the bottom right) has an identical shape. It is also important that disturbances in

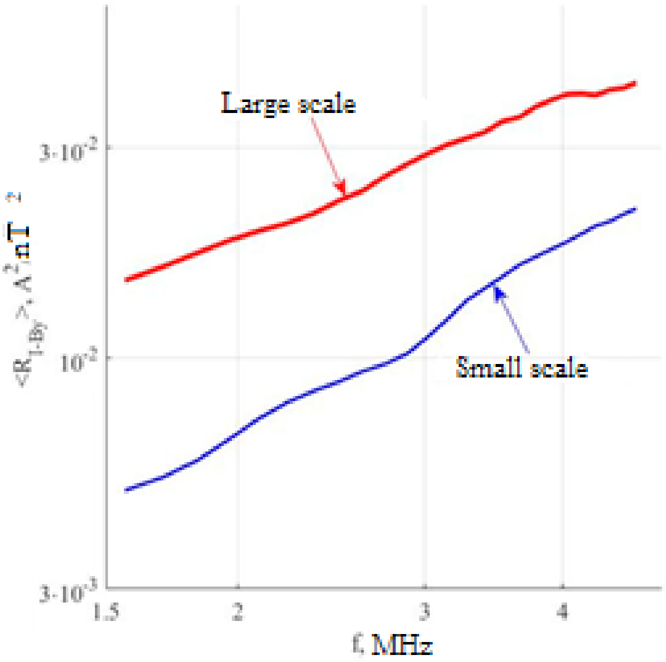

Pic. 7. Dependence of the ratio of the GIC amplitude to the pulsation amplitude on its frequency for different spatial scales of pulsations [44].

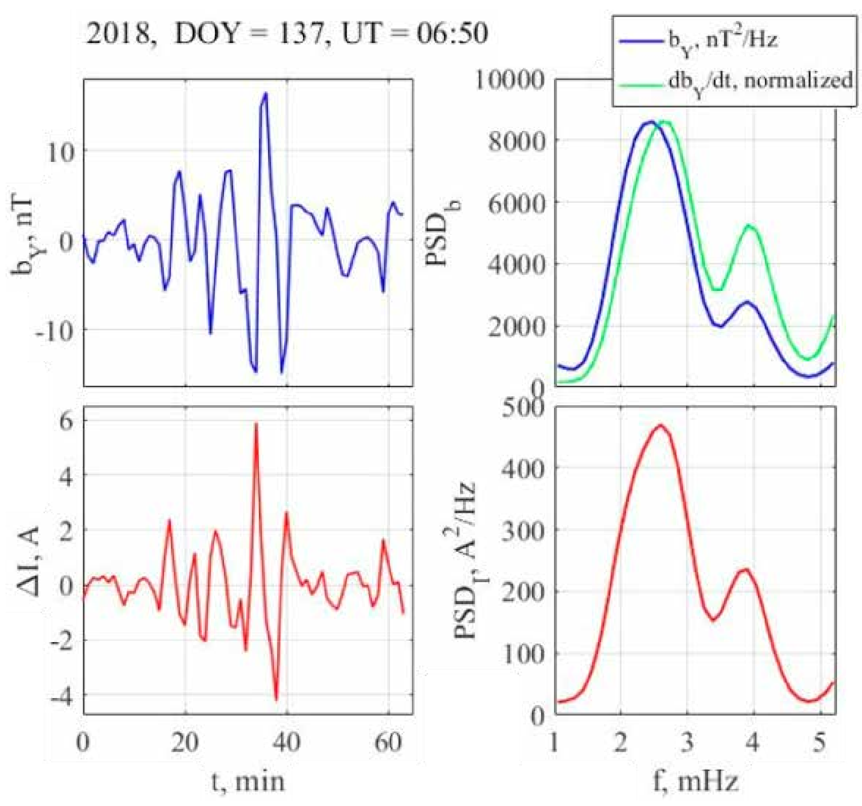

Pic. 8. An example of an exact match between the temporal shape (left) and spectra (right) of geomagnetic field pulsations (top) and GIC (bottom). The top right graph shows the perturbation spectra of the Y-component of the geomagnetic field and its time derivative m [45].

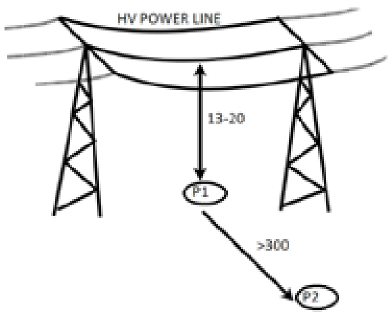

Pic. 9. Scheme of remote registration of GIC in power lines by differential method. P1 and P2 are the points of location of magnetometers, the distances are given in meters [compiled by the authors].

the geomagnetic field and in the GIC also coincide in time (graphs on the left).

The analysed intervals of Pc5/Pi3 pulsations recorded simultaneously in the geomagnetic field and GIC showed that for a power line extended in the meridional direction, the relationship between the spectral power of geomagnetic pulsations and GIC is stronger for the latitudinal (*Y*) than for the meridional (*X*) component of the geomagnetic field. This translates into both a higher correlation coefficient and a larger linear regression coefficient. In other words, the transverse polarisation of pulsations with respect to the strike of a power line has the greatest effect on generation of GIC in it [21].

Based on the analysis of three selected factors, it follows that, at high latitudes, off-storm pulsations with insignificant amplitudes are an important source of potentially dangerous GIC with amplitudes of several tens of A. Indeed, as follows from Pic. 8, the maximum range of pulsation amplitudes of only 25 nT leads to generation of GIC with an amplitude of 10 A. Recall that 25 nT is the characteristic amplitude of the quiet daily variation of the geomagnetic field at middle latitudes. The duration of the investigated pulsations can reach several hours. Such a long-term effect of GIC of ~10 A on the power supply system is statistically more dangerous than single bursts of GIC of ~100 A in the neutral that occur during storms and substorms.

1.4. Prototype of autonomous gradient installation for remote registration of GIC

Direct measurements of current in the neutral of transformers are technically complex, require high costs and physical connection to the transformer equipment, which is not always possible. In this regard, remote methods for detecting quasi-direct currents in high-voltage power lines are extremely promising and in demand for estimating the GIC value. This method is currently being widely tested and implemented around the world. The first experiments were carried out in 2016 in South Africa [46], and then the measuring installations based on this method were installed and tested in the UK, Spain, Portugal, and other countries [47–50]. The idea of the method is to install two three-component magnetometers in close proximity to power lines. The first magnetometer is installed under the line, and the second – at a distance of 100 to 300 meters (Pic. 9).

The calculation of the difference between the records of magnetometers makes it possible to eliminate natural perturbations and obtain variations in the total magnetic field vector from direct current in the power line. Applying the Biot-Savart law, which determines the induction vector of the magnetic field generated by a direct electric current [51], the direct current (GIC) in a power line is calculated by the formula:

(a) (b) (c)

Pic. 10. Observatory tests of sensors: field measurements of the field gradient (a), installation in the variation pavilion together with a standard high-precision vector magnetometer (b), one of two magnetometers of the gradient installation (c) [authors' photo].

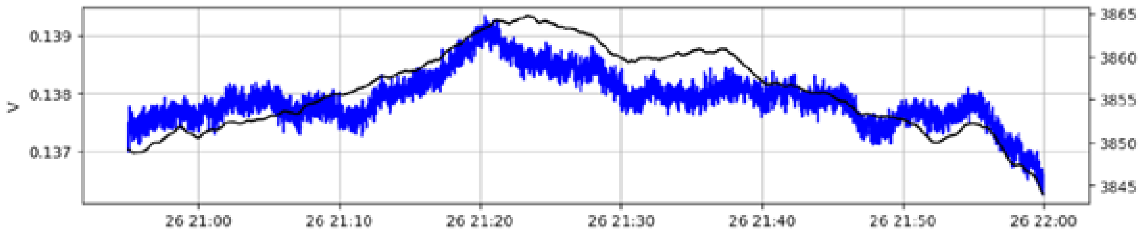

Pic. 11. Recordings of the eastern Y-component of the geomagnetic field with a gradient setup (blue [composite] curve, scale on the left, V) and an observatory magnetometer (black [single-line] curve, scale on the right, nT) [prepared with participation of the authors].

$$B = \frac{\mu_0 I}{2\pi R},$$

where B – measured field, R – distance to current conductor.

We are developing an installation based on the described method. Sensors based on a microstrip resonator with a thin magnetic film were chosen as magnetometers. At the magnetic observatory of the State Center of the Russian Academy of Sciences «Klimovskaya», Arkhangelsk region [52; 53], three-component assemblies of these sensors were tested (Pic. 10).

A comparison of these sensors with the standard set of magnetometric equipment of the observatory confirmed that sensitivity and accuracy of sensors are sufficient to measure the currents that occur during the flow of medium and strong geomagnetic disturbances (Pic. 11). As mentioned above, potentially dangerous GIC are characterised by short-period variations in the horizontal components of the magnetic field from 10 nT. Currently, a field version is being developed for testing in real conditions on the Northern Transit power line (Republic of Karelia and Murmansk region), equipped with a GIC measurement sensor through the transformer neutral. A necessary step will be calibration of the gradient installation for normal current in the electric power system under study.

2. Study of large geological structures and sedimentary basins based on a comprehensive analysis of geological and geophysical data

The importance of studying sedimentary basins in the Russian Arctic is due to the large reserves of minerals (primarily hydrocarbons) in this region. The research results provide new information for prospecting and exploration of oil and gas fields in the continental part and on the shelf in the Russian Arctic. Search, exploration, and development of hydrocarbon deposits require development of the necessary transport infrastructure in the region at a sufficient level. This section presents the results of studying large geological structures, sedimentary basins and geoinformation products built on their basis. Undoubtedly, these results should be considered in development and design of new transport routes in the Russian Arctic, which are necessary for implementation of projects both at the stage of exploration of deposits and at the stage of their operation.

The Mohorovichich (Moho) section is one of the most important boundaries in the bowels of the Earth, which is characterised by strong changes in all physical parameters, therefore, knowledge of the depths of the Moho section is extremely important for many geophysical models and for understanding the structure and dynamics of the lithosphere. Direct data on the Moho depth can only be obtained from seismic

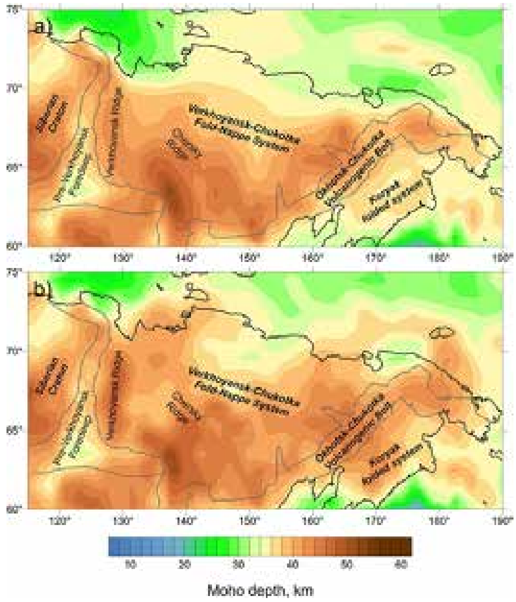

Pic. 12. Original Moho depth map (top) and corrected Moho map (bottom), depth from sea level [61] [prepared with participation of the authors].

surveys, the coverage of which is highly heterogeneous, and in the eastern part of the Russian Arctic, which is an extremely inaccessible territory, they are practically absent. A new Moho map was constructed for the eastern part of the Russian Arctic (region 60–75° N, 110–190° E) [54]. This region was chosen as the least studied within the Russian Arctic, and therefore is of particular interest. The map is based on the joint inversion of various geophysical fields, primarily the field of residual anomalies and vertical gravity gradients. The original map [55] was corrected according to these fields with additional restrictions from several seismic profiles. The new Moho model (Pic. 12(b)) has been compared in detail with the original model (Pic. 12(a)) and demonstrates some fundamental features that were absent before.

Thus, in the new model, under the Verkhoyansk Ridge, there is a lithospheric root 47 km deep compared to the relatively small Moho depression in the original model. A significant difference was found in the Moho depth (from 25–40 to 38–45 km) in the northern continental part of the study area and on the shelf. We suggest that this thickening of the Earth's crust is related to underplating due to plume activity that took place earlier. New information was also obtained on the Moho depth in the water area of the Chukotka microcontinent and under the location of Anadyr-Koryak fold system.

The structure of sedimentary basins was studied in the same East Asian Arctic zone. As a result of calculation of gravity decompensation anomalies, a new sedimentary thickness model for the eastern sector of the Russian Arctic [56] was obtained, which demonstrates new significant details about the structure, area, and density of sedimentary basins in comparison with the results of geological studies. In particular, new data on the thickness of the sedimentary cover were obtained for Zyryansk, Anadyr, Chaun, and other sedimentary basins (Pic. 13).

For the circumpolar Arctic, a new model of geothermal heat flow was obtained based on inversion of seismic and magnetic data [57]. To construct a new heat flow map for the region under study, the catalogue of the International Heat Flow Commission and two theoretical predecessor models [58; 59] were used. Pic. 14 shows a comparison of compilation of the original models (Pic. 14(a)) with the new model (Pic.14(b)). The new map reveals some features that have not been previously identified – in particular, zones of increased heat flow in the Bering Strait, the Chukchi Sea and a residual anomaly in the Labrador Sea region associated with the Paleogene-active Mid-Labrador Ridge. An increase in heat flow in the ancient rift zone that separates Eastern and Central Siberia is also visible.

Also, models of the elastic characteristics of the lithosphere were built – flexural stiffness (Pic. 15 (a)) and effective elastic power (Pic. 15 (b)) for the lithosphere throughout the Arctic zone of Russia. In this study, we used the method for determining the elastic parameters of the lithosphere [60]. It is based on cross-spectral analysis of data on the gravitational field and near-surface load. An important addition compared to previous works was the use of not only topography data as a surface load, but also the density inhomogeneities of the sedimentary cover. A refined model of these inhomogeneities was obtained in [56].

As a result of the work done, a collection of geophysical fields for the Russian Arctic was published [61], which includes the above-described results of modelling the Arctic lithosphere, as well as a number of data collected from open sources (for example, sections of seismic tomographic models of the Arctic before the division between the upper and lower mantle). In the course of research in this area, the following digital data arrays were additionally obtained:

- Gravitational effect of the crust and upper mantle (gravitational field and its vertical gradients).
- Residual «mantle» gravity anomalies similar to vertical gradient anomalies and residual topography (1^ox1^o resolution).
- Density model of the consolidated crust (1^ox1^o resolution).
- Corrected upper mantle model: mean density values for the Moho layers –75 km, 75–125, 125–175, 175–225, 225–275 and 275–325 km on 1^ox1^o grids.
- Changes in density due to variations in temperature and variations in mantle composition.

3. Assessment of seismic activity in the Russian Arctic

The Russian Arctic today is a poorly studied region in terms of seismic hazard assessments. Estimates for different parts of this region in some cases differ significantly from the real situation [62]. At the same time, accounting for

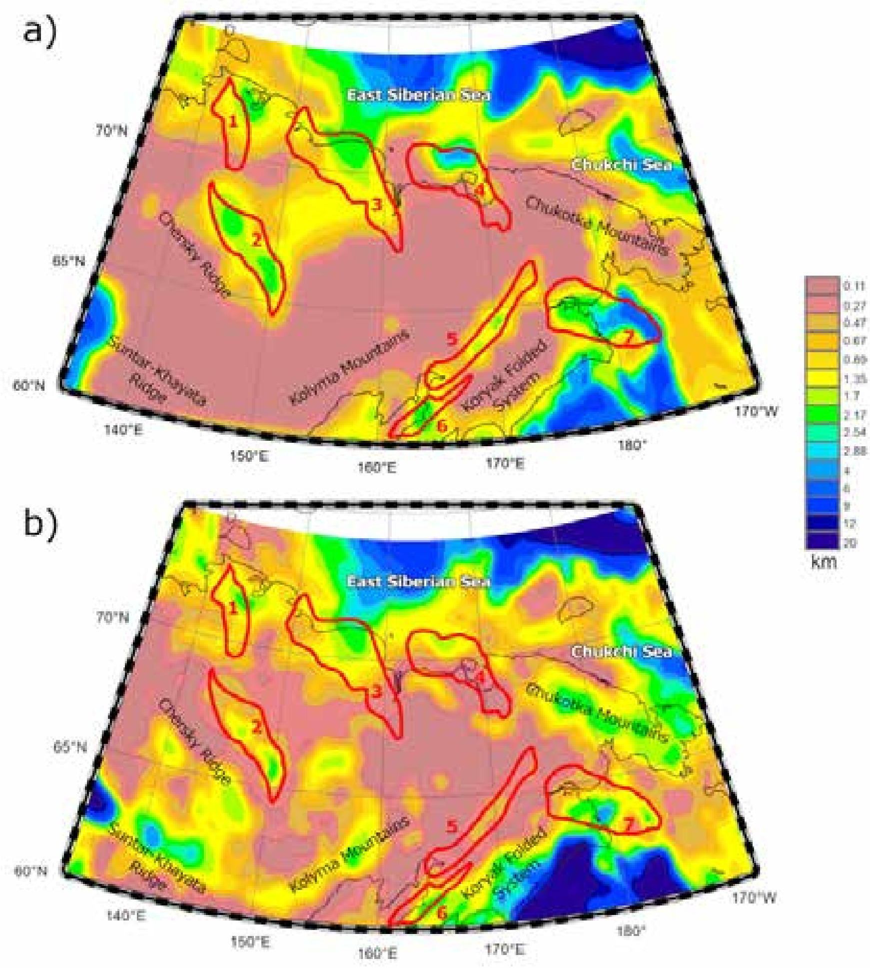

Pic. 13. The original sedimentary cover model (top, a)) and the new sedimentary cover model obtained using the decompensation anomaly approach (bottom, b)). Red contours with numbers indicate the analysed sedimentary basins: 1 – Tastakhsky, 2 – Zyryansky, 3 – Primorsky, 4 – Chaunsky, 5 – Penzhinsky, 6 – Pustoretsky, 7 – Anadyrsky [61] [prepared with participation of the authors].

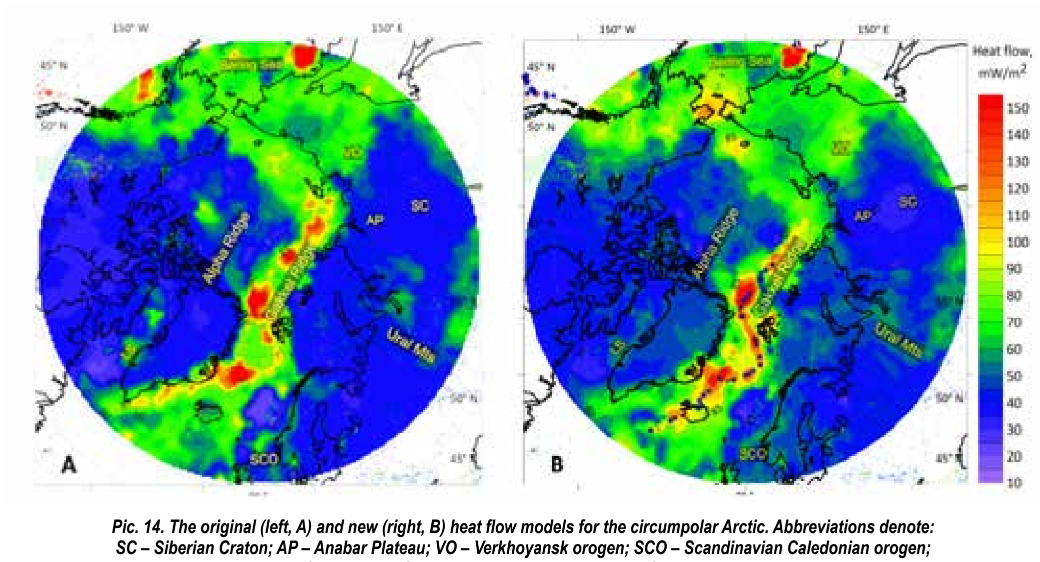

Pic. 14. The original (left, A) and new (right, B) heat flow models for the circumpolar Arctic. Abbreviations denote: SC – Siberian Craton; AP – Anabar Plateau; VO – Verkhoyansk orogen; SCO – Scandinavian Caledonian orogen; LS – Labrador Sea [prepared with participation of the authors].

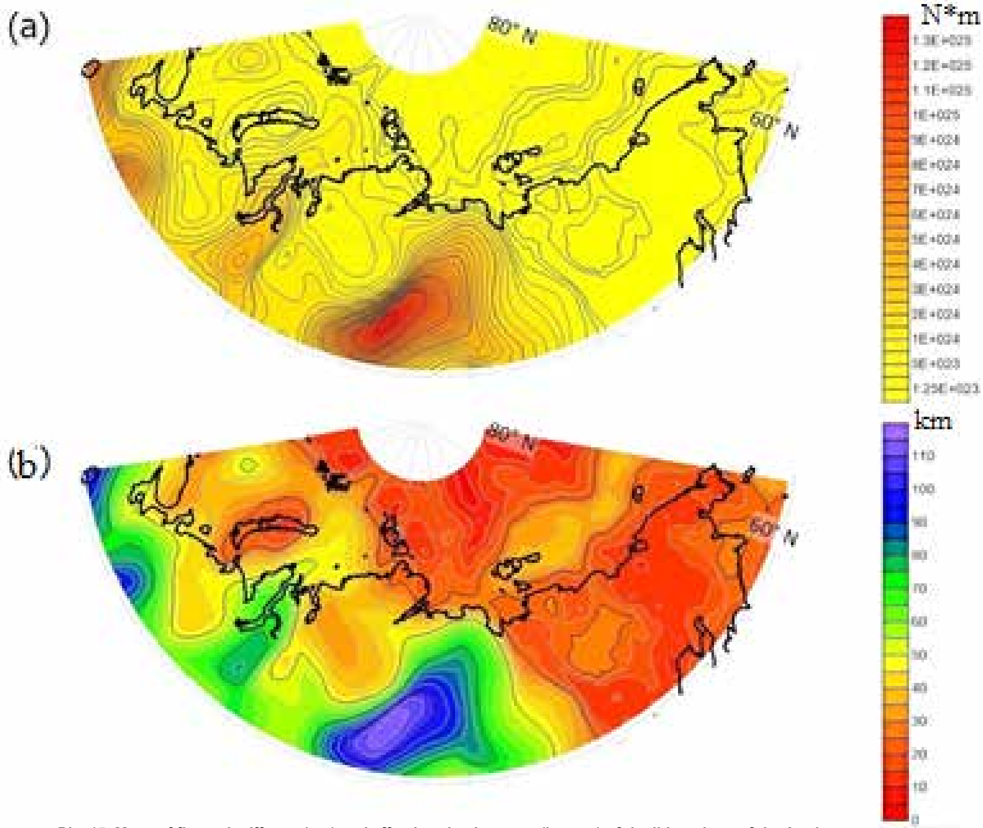

Pic. 15. Maps of flexural stiffness (top) and effective elastic power (bottom) of the lithosphere of the Arctic zone of the Russian Federation [prepared with participation of the authors].

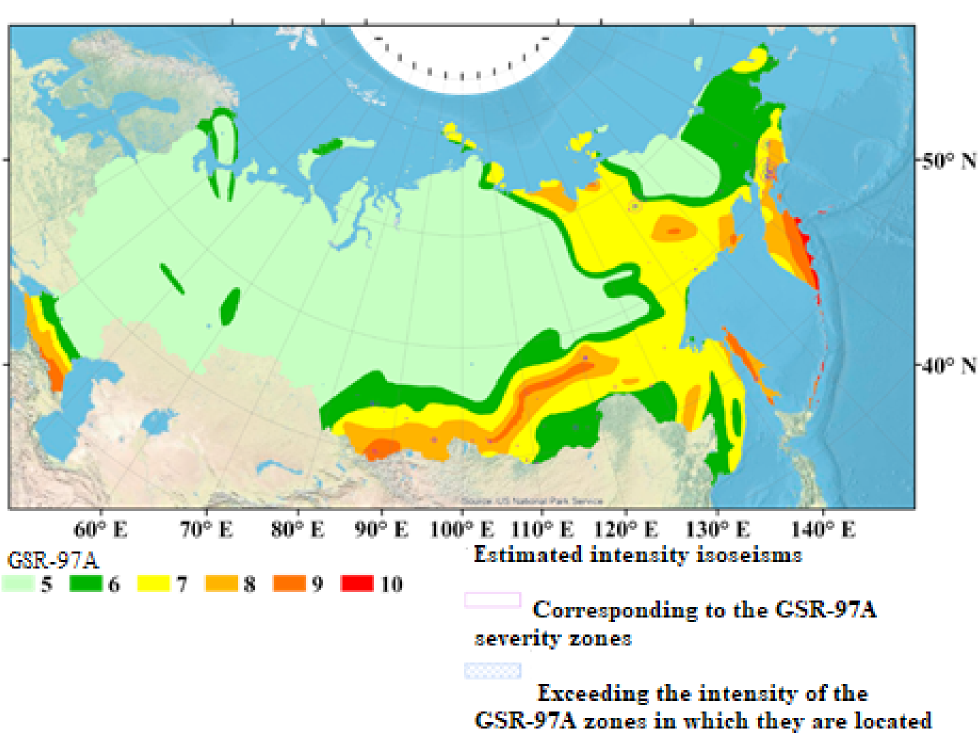

Pic. 16. GSR-97A map and calculated theoretical isoseisms [62].

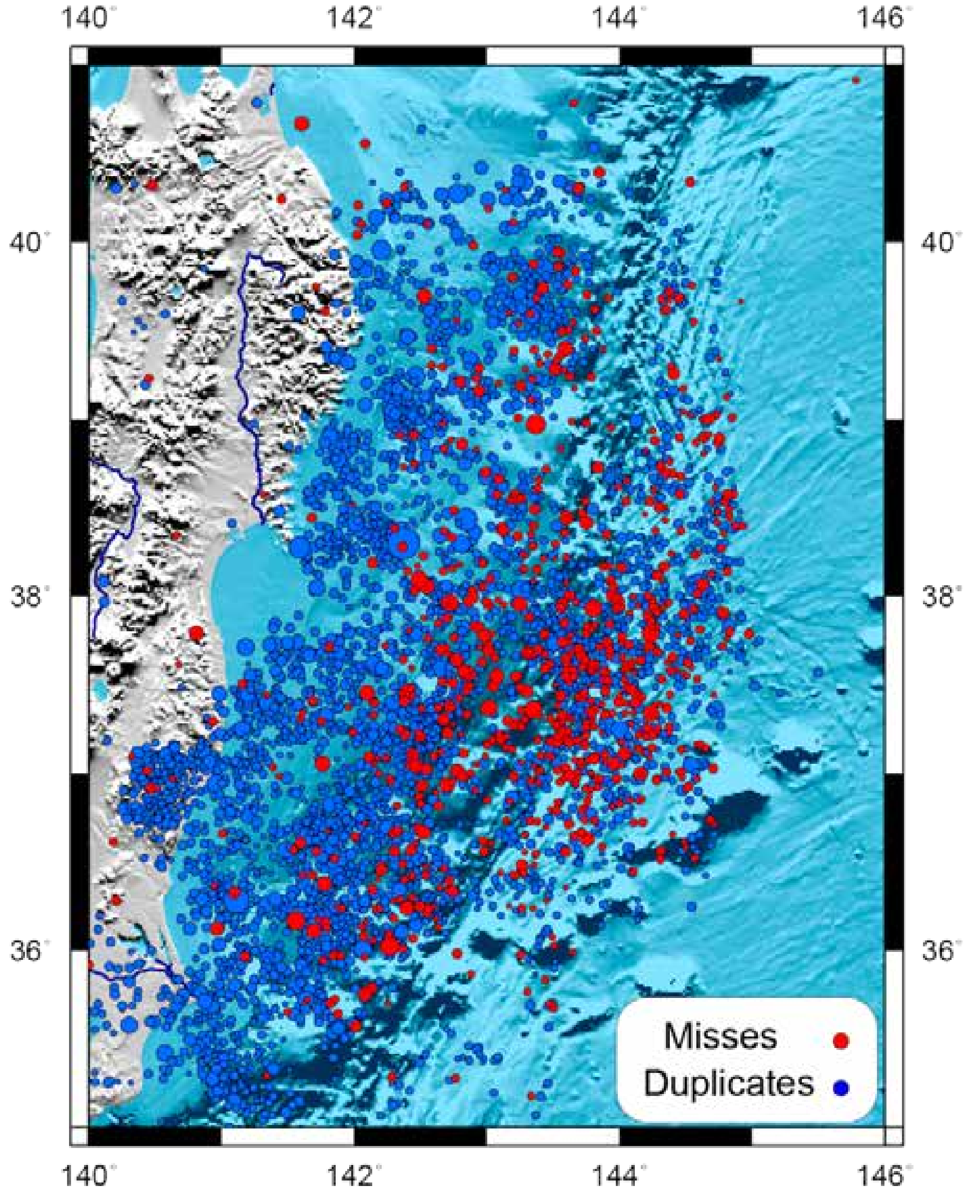

Pic. 17. Epicentre map of the ANSS catalogue of the aftershock sequence of the 2011 Tohoku earthquake. Events missing in the JMA catalogue are shown in red [developed with participation of the authors].

seismic activity plays a critical role in operation, planning and development of transport systems in the region. In this regard, the task of creating a system-analytical complex for recognising signs of places of possible occurrence of dangerous seismic and other geodynamic events in the Arctic and calculating seismic hazard and seismic risk for given territories and objects is relevant. Particular attention is paid to the study of such linear objects as railways, highways, power lines and pipelines.

As an initial step in recognising zones of possible occurrence of strong earthquakes in the AZRF, a numerical comparison of the maps of the General Seismic Zoning (GSR) [63] was carried out with the impact from earthquakes that actually took place after publication of the maps. A comparison was made of the area of zones of expected intensity on the GSR-97A map with the area of isoseisms from actually occurred earthquakes. The study showed that the isoseism area is, on average, an order of magnitude smaller than expected according to the GSR-97A map (Pic. 16). Thus, in most regions of Russia, assessment of seismic hazard on average can be overestimated by at least 10 times. This observation is especially important for the Russian Arctic, where, against the background of a very weak actual seismic impact, significant areas of the Kola Peninsula, the Novaya Zemlya and Severnaya Zemlya archipelagos, the New Siberian Islands, the Taimyr Peninsula, as well as the north of Yakutia and Chukotka are assigned to zones with an intensity of 6 and higher. In the article [62], ways were proposed to improve seismic hazard assessments necessary for a systematic analysis of geophysical processes in the Arctic.

In the process of preparing the most complete catalogue of earthquakes in the Russian Arctic, the authors and their colleagues identified significant differences in the catalogues of the International Seismological Centre (ISC) and the Single Geophysical Service of the Russian Academy of Sciences (EGS RAS). In this regard, the ISC catalogue was supplemented with events from the EGS RAS catalogue and other Russian local sources. For this, an original algorithm for combining earthquake catalogues was created, the main task of which is to identify the resulting duplicates and separate them from aftershocks. The algorithm is based on the authorial modification of the nearest neighbour method [64; 65] for takes. Its ideological basis is the fact that, unlike aftershocks, duplicates do not have a causal relationship. For events from two catalogues, a one-to-one correspondence is built, after which the classification of earthquakes into unique and duplicates is performed using the Euclidean metric of the «Frolich type». Thus, the developed algorithm makes it possible to automatically combine any number of earthquake catalogues [66].

The efficiency of the algorithm was first demonstrated by combining the ANSS (USGS) and JMA (Japan Meteorological Agency) catalogs of the aftershock sequence of the 2011 Tohoku earthquake (Pic. 17). Later in 2021–2022 the algorithm was developed and modified for its direct application to AZRF data.

As a result, for the first time in 2022, the most complete integrated catalogue of earthquakes in the eastern part of the Russian Arctic was created [67] and two catalogues, in their unification covering the entire western part of the Russian Arctic: the integrated catalogue of the western sector of the Russian Arctic and the catalogue of the Gakkel Ridge [68]. All three authorial catalogues are provided with their own single magnitude scale. The catalogues of the western sector of the Russian Arctic and the Gakkel Ridge are divided into two sets ordered by time, since their single magnitudes are mutually incompatible.

Pic. 18 shows the events from the created combined catalogues for the western and eastern sectors of the Russian Arctic, which integrate all available seismic data from ISC, Russian regional catalogues of the EGS RAS and a number of other sources. The catalogue of the eastern sector of the Russian Arctic (Pic. 18(b)) contains 23254 events for 1962–2020, of which 7781 are from ISC and 15473 are from Russian sources [69]. For the created catalogue of the western sector of the Russian Arctic (Pic. 18 (a)) the work was carried out to identify and remove explosions and other events that are not earthquakes. For the period 1998–2020, when all such events were deleted with a high degree of certainty, the catalogue contains 2126 entries. In total, for the period 1963–2022, the catalogue contains information on 4629 seismic events. The Gakkel Ridge catalogue contains about 17000 events.

Further studies were related to the spatial assessment of seismic activity using data from the created earthquake catalogues. As a measure of energy, the authorial modified magnitude indicated above was used. For the eastern sector of the Russian Arctic, the values of the coefficients of the Gutenberg-Richter law of repeatability were calculated on a regular grid with a step of 0.1^{o} in latitude and longitude. Pic. 19 (a) shows a map of local values of the representative magnitude. Based on these data, the boundaries of the region were determined, in which the value $Mc = 3.0$ can be taken as a representative magnitude. In the rest of the region, this value is $Mc = 4.0$.

The nearest neighbour method was used to divide the catalogue into background and dependent events. Further evaluation of seismicity parameters was carried out using the catalogue of background events. On a grid with a step of 0.1° in latitude and longitude, the seismic activity parameter $a(m4) = log_{10}v$ was calculated, where v is an estimate of the number of earthquakes with a magnitude $M \geq 4.0$, calculated considering the fractal dimension of distribution of epicentres. As a result, maps of variations in the slope of the recurrence plot (b-value) (Pic. 19 (b)) and the seismic activity parameter $a(m6) = a(m4) - 2b$ (Pic. 19c) were constructed. According to the method [70], the productivity of each earthquake was calculated

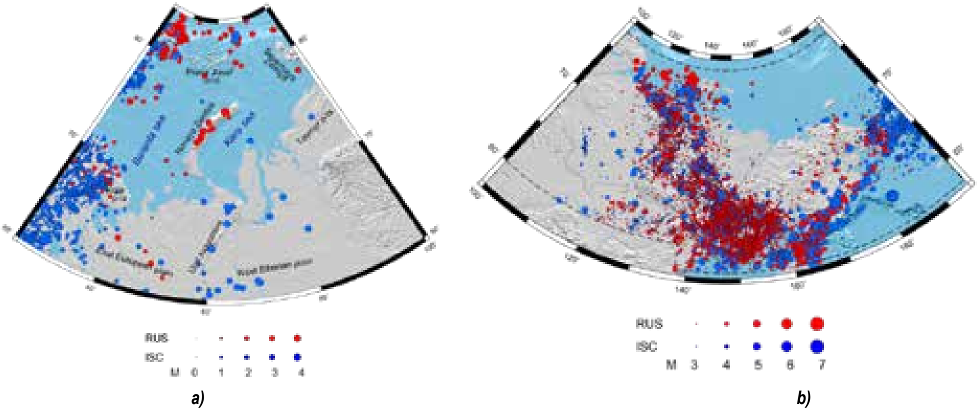

Pic. 18. Maps of the epicentres of the combined catalogues of the Russian Arctic: (a) the western sector for the period 1998–2020; (b) Eastern sector for the period 1962–2020. Blue indicates earthquakes from the ISC catalogue, red indicates events from Russian and other sources [compiled with participation of the authors].

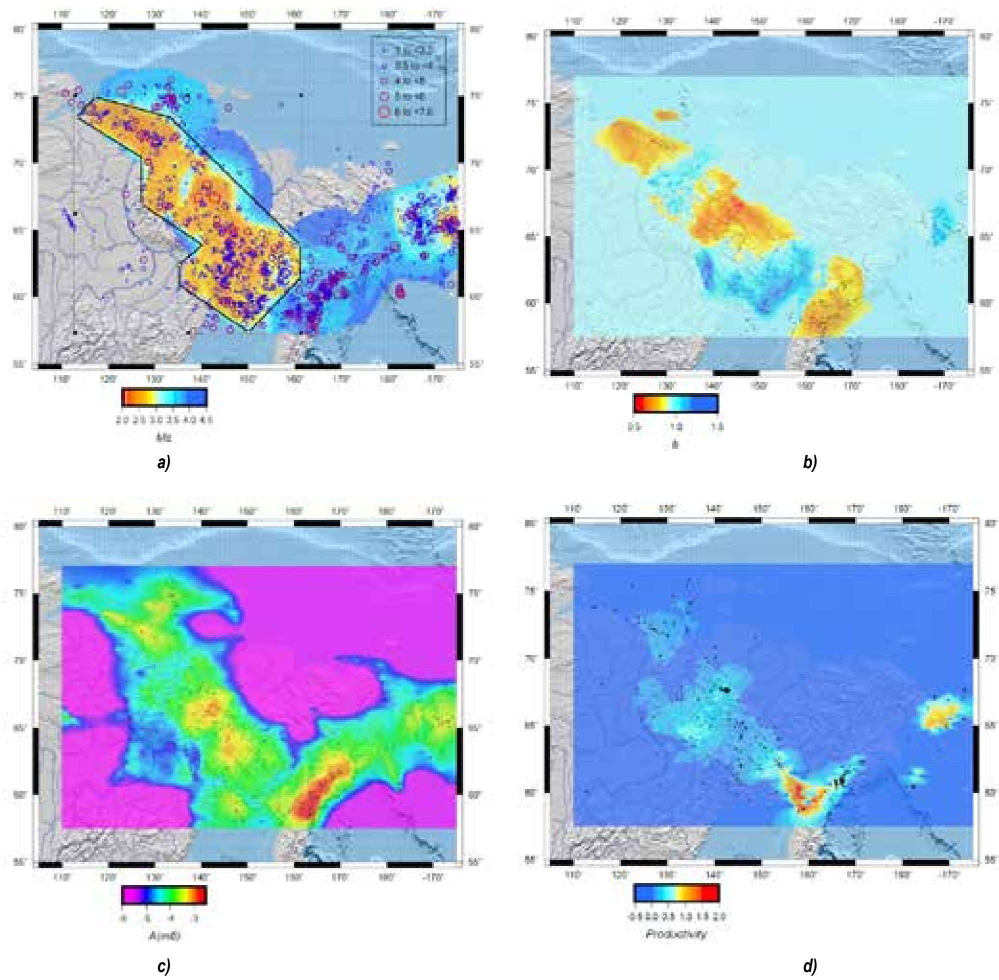

Pic. 19. Estimation of seismic activity in the eastern sector of the AZRF according to the integrated earthquake catalogue of the AZRF [prepared with participation of the authors]:
(a) – map of the magnitude of the full registration of Mc for the period 1982–2020, built by the multiscale method (the polygon marks the area where earthquakes with M ≥ 3.0 are used to calculate the seismicity parameters, earthquakes with M ≥ 4.0 are used in the rest of the territory);
(b) – variations in the slope of the recurrence plot (the values of b – value are tied to the average position of the earthquakes in the sample; R = 300 km, Nmin = 50 events; in places of low seismic activity, the regional value of the slope of the recurrence plot b = 0.924 is used);
(c) – seismic activity a(m6) on a logarithmic scale (variations in seismic activity for any magnitude level are calculated in accordance with the local value of the slope of the recurrence graph a(M)=a(Mc) –b(M–Mc);
(d) – average productivity in circles with radius R = 300 km, DM = 1 (black circles mark the earthquake epicentres used to calculate productivity).

in the band of magnitudes $DM = 1$. As a result, in circles with a radius of $R = 300$ km, the values of average productivity were calculated and mapped (Pic. 19 (d)). This made it possible to determine regional estimates of parameters of the Omori-Utsu law, according to which a GIS-oriented database was formed.

To model the seismic process in the region under study, it is useful to use a synthetic catalogue of earthquakes. Such a catalogue is a new artificially created set of analogues of seismic pseudo-events generated by analogy with the records of a real catalogue. A synthetic catalogue reproduces the main properties of a real catalogue and is generated for an arbitrary time interval. We have developed a method for constructing a synthetic catalogue of earthquakes, which is based on the synthesis of three groups of approaches to assessment of geodynamic hazard. The main idea of the method is the assumption that the Gutenberg-Richter law is fulfilled at the regional level, and possible local deviations are compensated for by averaging over the entire region. Therefore, times and magnitudes of background events in the synthetic catalogue are determined for the entire region, regardless of their location. The parameters of pseudo-events are generated in accordance with the regional law of recurrence, and their location is determined as a vector random variable with a given spatial distribution depending on the magnitude. The distribution is constructed for each magnitude value based on local estimates of the Gutenberg-Richter law.

Another important assumption is that the strongest earthquakes occur in a limited number of zones within the region under consideration. To determine these zones, recognition methods based on a system analysis of the region's earthquake catalogue, FCAZ recognition, were used [71]. The latter study is of great independent importance both for clarifying the seismic zoning of the Russian Arctic and for orienting the planning of construction of high-risk facilities, including highways, sea and river ports, airports, railway, and bus stations, etc.

Thirdly, aftershocks make a significant additional contribution to the overall seismicity and seismic hazard. The ETAS model [72] is used as the basis for stochastic aftershock modelling. In this model, the seismic regime is interpreted as a superposition of sequences decreasing in time according to the Omori-Utsu law. The spatiotemporal variant of the ETAS model [73] considers the power law of decrease in intensity of aftershocks with distance from the epicentre of the main shock. ETAS postulates that the number of aftershocks for earthquakes of the same magnitude is the same. However, the recently established law of earthquake productivity [70] refutes this postulate, at the same time explaining the fact that the intensity of the earthquake flux predicted for future time intervals by the ETAS model is overestimated. The applied method uses the ETAS-e model [70; 74], which additionally considers the law of earthquake productivity. This model corrects the main drawback of the ETAS model [74]. Using this method, a synthetic catalogue of earthquakes was prepared for a conditional period of 1000 years for the eastern sector of the Russian Arctic.

Recognition of the places of possible occurrence of strong earthquakes with $M \geq 5.5$ in the eastern sector of the Russian Arctic was performed using the above-mentioned FCAZ algorithm [69; 75]. Earthquake epicentres from the integrated earthquake catalogue of the Russian Arctic were used as recognition objects (Pic. 18 (b)). The choice of the magnitude threshold, starting from which the epicentres were used as objects of FCAZ-recognition, was carried out on the basis of the analysis of frequency graphs. The recognised FCAZ zones are in good agreement with the location of the epicentres of historical and instrumental strong earthquakes (Pic. 20) and are mainly confined to the boundaries of the Eurasian, North American, and Sea of Okhotsk tectonic plates. In the zone of contact of all three plates and the Sea of Okhotsk with the North American, very large FCAZ-zones were identified, containing half of the strong earthquakes known in the region. FCAZ zones are also recognised within the Chersky Ridge, which is one of the main geological structures in the region. A fairly large number of instrumentally recorded strong earthquakes are known within the boundaries of this ridge [67].

4. Geoinformation support for system analysis of geophysical processes in the Russian Arctic

An effective tool for complex analysis and combined visualisation of new geological and geophysical data obtained about the Arctic region are geographic information systems (GIS). It is important that this provides high-level storage of geographic objects using an object-relational

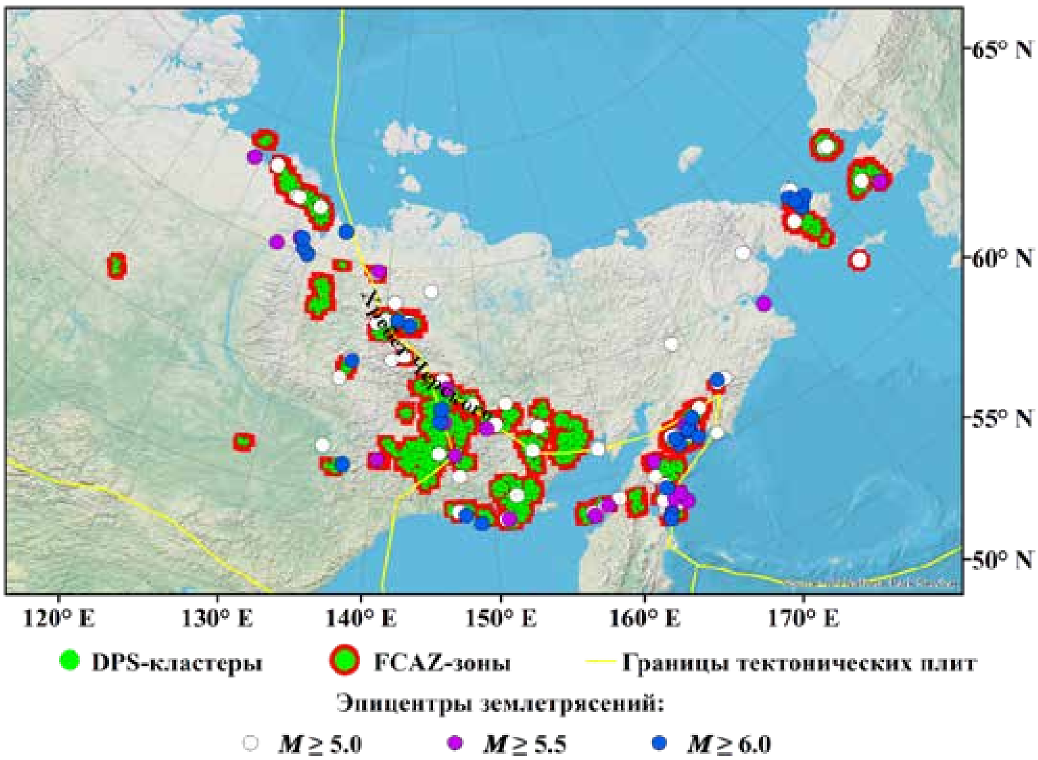

Pic. 20. FCAZ zones of possible occurrence of earthquakes with M ≥ 5.5 in the eastern sector of the Russian Arctic and epicentres of earthquakes with M ≥ 5.0. The map can be recommended for the use as a reference during further construction and operation of transportation roads [developed with participation of the authors].

database management system. The use of modern technologies of geoportals makes it possible to provide interactive online access to the obtained scientific results to a wide range of researchers. High-quality visualisation is a powerful tool in the field of modelling and systems analysis and, as a result, becomes an important part of processing and management of large amounts of data.

The studies described in the previous sections systematically generate new data in the following major scientific areas: geomagnetism and space weather, the structure of the earth's crust, and seismic activity. As they are received, a common, integrated database of geospatial data on the Russian Arctic is expanding. For example, geothermal heat flow modelling data, calculated as part of the study of the structure of the earth's crust in the Arctic, depth maps of the main geological boundaries (Mohorovichich boundary, upper mantle, sediment bottoms and lithosphere-asthenosphere boundary) were added to the database, which were used in the calculations of this new model, the initial thickness of the sedimentary cover, based on the compilation of these models for water areas and land, the effective elastic thickness of the lithosphere, the integrated catalogue of earthquakes in the Russian Arctic, and many others.

Any auxiliary geological and geophysical information involved in the course of research is also included in the database. Such data, for example, include data on geology (forecast mineralogical map at a scale of 1:2 500 000, a geological map at a scale of 1:2 500 000, a map of the thickness of the sedimentary cover), geodesy (a topographic map of the Russian Federation at a scale of 1:1 100 000); ETOPO and GEBCO digital elevation models), hydrology (maps of redistribution of snow volumes, temporal variability of snow cover, groundwater runoff, total river runoff, snow stock, river runoff variations, meltwater runoff, potential ice cover, establishment and melting of snow cover), networks geophysical observations (maps of distribution of observatories and stations of geophysical observations), glaciology (maps of the boundaries of permafrost, the degree of glaciation of territories, the thickness of the ice cover, the temperature regime in the permafrost zone), mineral deposits (maps of large and unique mineral deposits), soil science (maps of classes and types of soils), geophysics (maps of the Earth's anomalous magnetic field; earthquake

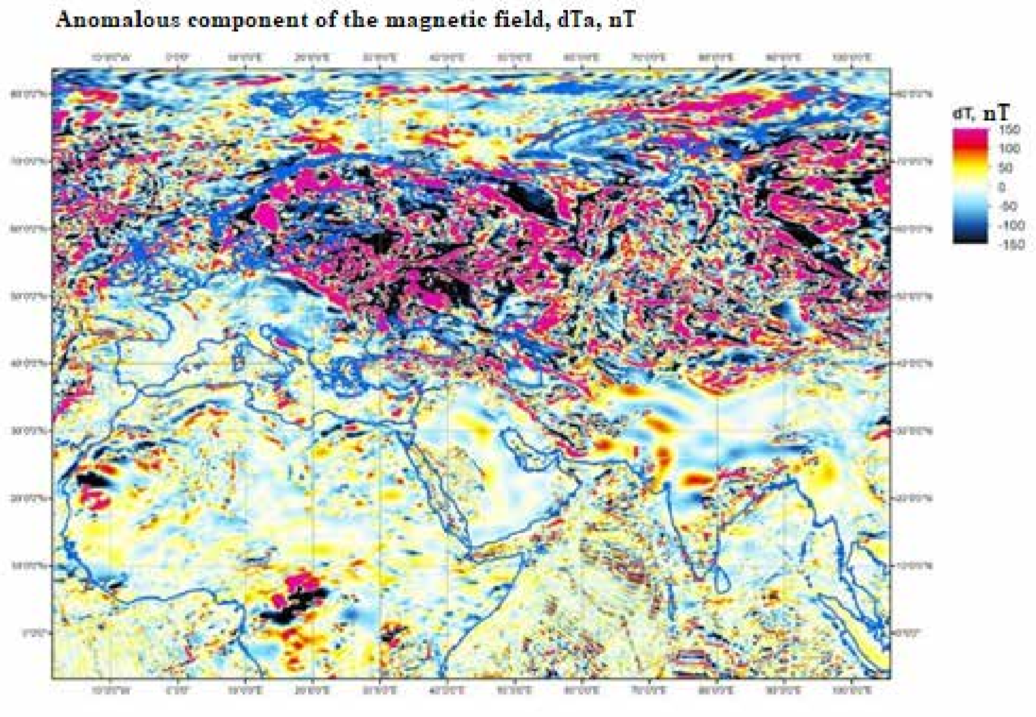

Pic. 21. Fragment of the map of the anomalous component of the magnetic field, constructed according to the model [76] with participation of the authors.

epicentres; geoid anomalies; gravity anomalies; depths to the Mohorovichic surface; seismic wave velocities, etc.), biogeography (maps of swampy areas, vegetation, bioclimatic zones and vegetation zones). As an example, Pic. 21 shows GIS data layers on the Earth's lithospheric magnetic field according to the model of field expansion in spherical harmonics up to the 1050 degree [76]. The model was built based on magnetic field measurements from the CHAMP and Swarm satellites, as well as data on near-surface scalar anomalies obtained during local marine and terrestrial surveys of the magnetic field. The final data are presented for the entire planet with a step of 0,1° in latitude and longitude. The geodatabase includes information about the anomalous magnetic field and its three orthogonal components. For each of the components there is a variant of the field at a height of 0 kilometres, and recalculated to a height of 5 kilometres.

Additionally, in the specified GIS-repository, the section «Directions for development of the Arctic» was created, containing spatial information about the already created and planned infrastructure facilities of the Russian Arctic. The data layers presented in this section were compiled in accordance with Decree of the President of the Russian Federation of October 26, 2020, N 645 «Strategy for development of the Arctic zone of the Russian Federation and ensuring national security for the period up to 2035» and include transport facilities (ports, airports, roads, and railways), energy facilities, developing tourist facilities, objects of science and education. Now, the database includes more than 200 layers of geodata in 46 categories.

For wide access to the accumulated data, the Arctic geoportal (https://arctic-gis.gcras.ru/) with an extensive user interface was developed and continues to be developed. Among other things, the following tools for interacting with spatial data have been added to it: «Measuring distances», which allows measuring the linear distance between two or more objects, as well as measuring the area of spatial objects; «Coordinates», which allows clarifying the coordinates of an object on the map; «Selection», which allows selecting a specific type of data within one category, and also provides the output of an attribute table containing only the type of data that the user is interested in (Pic. 22).

The concept of interactive spherical visualisations (ISV) is the study of planetary

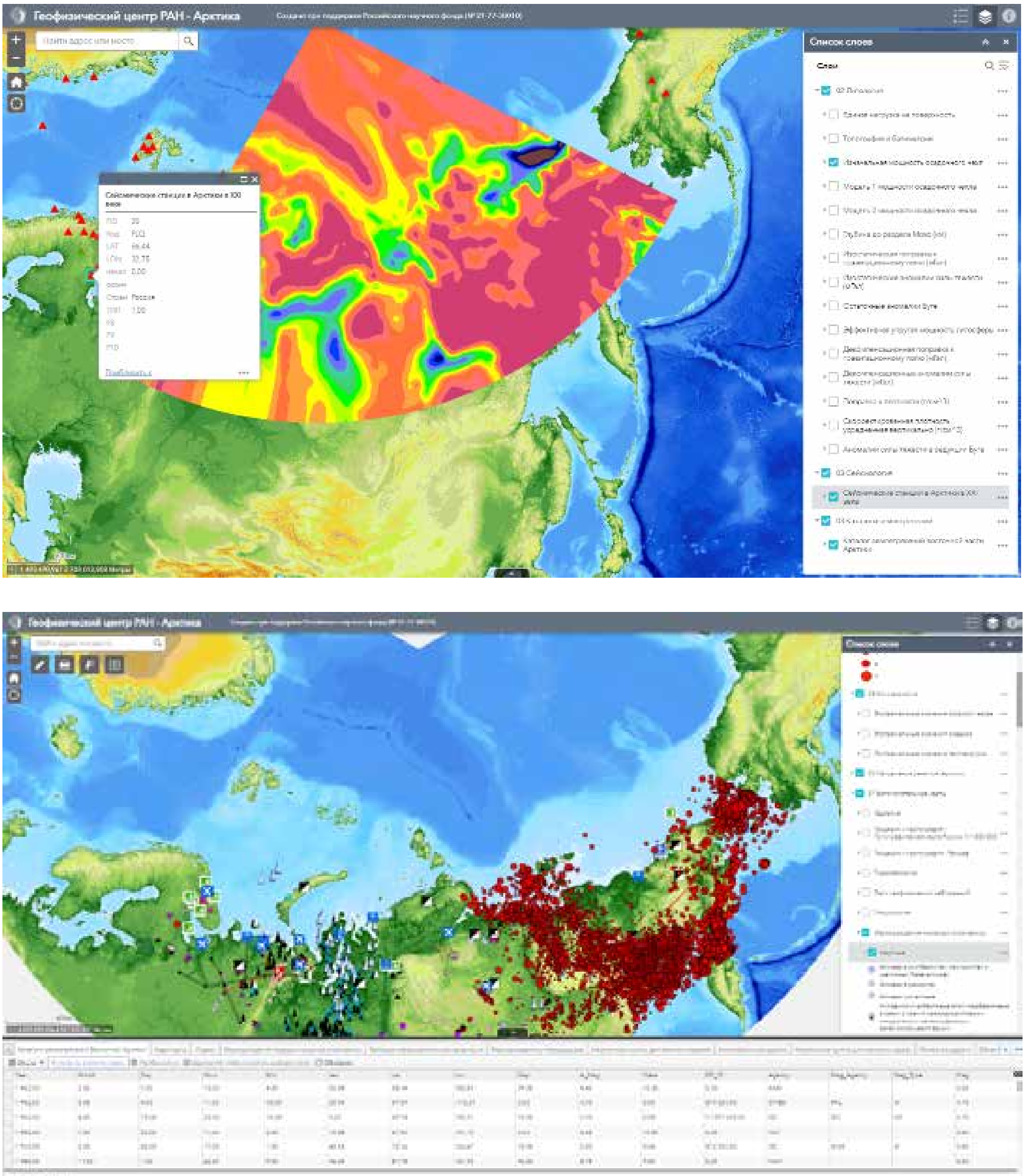

Pic. 22. General view of the interface of the geoportal «Arctic»: at the top – a map of the thickness of the sedimentary cover and a call to the context menu with attributive information about the selected seismic station; on the bottom – work with the attribute table of the layer with the catalogueof earthquakes in the Arctic. The list of available layers is shown in the menu on the right [portal screenshots provided by the authors].

processes and phenomena and their representative representation in an interactive form from a variety of devices without the use of specialised GIS tools. To date, ISV is being actively developed within the framework of the «Digital Earth» / «true-3D» paradigm in the areas of hardware and software systems with a spherical screen and virtual globes. At data.sph.gcras.ru, a public NAS-type file server was deployed based on the open LINUX operating system OpenMediaVault. The thematic data section for the Russian Arctic is located at data.sph.gcras.ru/Arctic. The server provides an access to structured source data for ISV clients via high-level FTP and SMB application protocols online. Additionally, the storage is an rsync server that allows synchronising files and directories according to a custom schedule. The prototype of a single ISV geographic information system was tested by playing spherical slides on ISV network through client-server interaction according to the principles of the developed architecture. On the example of organising thematic data on the Russian Arctic, the

(a)

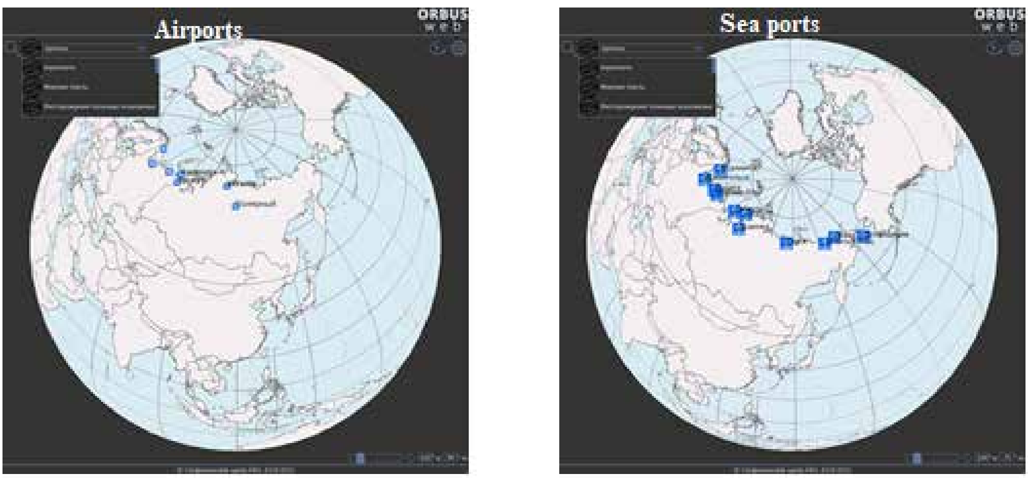

(b)

Pic. 23. Reproduction illustrations of ISV «Roads» and «Railways» presented using the ORBUS complex (a), as well as ISV «Airports» and «Seaports» made using the ORBUS Web (b) [provided by the authors].

architecture (a set of directories, files and principles of interaction with them) of the server part of the ISV system was implemented. The created file server organises single access to the content storage system for geovisualisation software technologies. The prototype of the ISV single geographic information system was tested by the ISV client applications developed at the GC RAS: the ORBUS hardware-software complex with a spherical projection screen (Pic. 23 (a)) and the ORBUS Web «virtual globe» web application (Pic. 23 (b)).

DISCUSSION AND CONCLUSIONS

The most active manifestations of geomagnetic disturbances are observed at auroral latitudes [77; 78], therefore, these factors pose a particular danger for safe operation of technological systems in the Russian Arctic, since the Russian Federation has the longest oil and gas pipelines, power lines and transport routes. Despite the exceptional importance of such studies, the influence of geomagnetically induced currents (GIC) on electric power systems and on the reliability of electrical equipment is still not considered in domestic regulatory documentation. While most space weather studies have focused on the impact on electrical networks, much less attention has been paid to disruption of the railway sector [79], although the mechanism of this impact has not yet been sufficiently studied [80].

At the same time, anomalies in train signalling and control systems associated with this phenomenon have been repeatedly documented [81]. The results presented in this article confirm that geomagnetic activity at high latitudes is a significant cause that controls the occurrence of failures in operation of railway signal automation [22]. The improvement of the technical base, aimed at ensuring smooth operation of railway signal, is accompanied by an increase in complexity of the technological infrastructure and leads to disappearance of some effects and emergence of new ones. However, the general physical cause of failures in operation of signal automation, associated with excitation of GIC in an extended conductor, cannot be eliminated.

The operation of transport systems also depends on other technologies potentially affected by space weather, such as power supply, communications, positioning, navigation and time synchronisation systems. Since during strong storms the impact of disturbances spreads quite widely and is of a planetary nature, it is necessary to coordinate efforts to predict space weather and develop measures to mitigate direct and indirect impacts of disturbances on systems and services associated with operation of transport systems [42].

The paper demonstrates that statistically weaker, but frequent and prolonged geomagnetic events generate more dangerous GIC, in contrast to rare but strong geomagnetic storms. The key factors affecting the GIC efficiency of these events are their spatial scale, spectrum shape, and polarisation. From the point of view of the negative impact of GIC on power supply systems, the geometry of the power transmission line and its orientation in space are of key importance. So, the greater is the length of a power line, the more intense are the induced currents that arise in it during geomagnetic activity, and this circumstance, of course, must be borne in mind when designing new networks. One solution, which is being applied in a number of Scandinavian countries, could be to split the power lines into shorter segments.

For a full-scale scientific substantiation of prevention of the negative impact of space weather on electric power networks, it is necessary to develop a GIC monitoring network. The paper proposes a promising autonomous installation based on gradient magnetometric sensors, capable of remotely measuring GIC excited in power lines. Based on the results of statistical and correlation analysis, it is shown that remote sensing of GIC in high-latitude power lines by observing geomagnetic disturbances is characterised by a relative error within 1,5 % of the range of GIC values for the study period. Thus, the introduction of such installations into a high-latitude observing network will make a significant contribution to the development of a system for assessing possible negative effects of space weather and a short-term forecast (for 0,5–1 hour) of the possibility of critical GIC levels. Such a forecast can be used by operators to take the necessary measures to reduce the risk of catastrophic consequences.

Studies of spatial distribution of GIC sources have shown that geographically they gravitate towards the equatorial boundary of the auroral oval, which makes it especially relevant to predict the intensity of precipitation of high-energy particles and the position of auroral oval boundaries. Such a forecast is also extremely important because the stronger is the disturbance, the lower are latitudes to which the equatorial boundary of the oval shifts. For these purposes, an online system was developed (http://aurora-forecast.ru) based on the OVATION-Prime empirical mathematical model and GIS technologies, which provides such a forecast with a horizon of 30–70 min and an efficiency of more than 86 %. In addition, the system performs computer simulation of the instantaneous position of the auroral oval and visualisation of spatial distribution of retrospective data. When displayed on a virtual globe, the studied parameters are superimposed on a digital map of main railway lines and other transport systems in Russia.

The long-term and operational forecast of availability of the required navigation characteristics for the period of the helio-geomagnetic disturbance is the most controversial and complex area of GNSS modernisation. The above information shows that extreme space weather factors can cause significant degradation of the quality of GNSS and their functional additions.

The results obtained allow drawing the following preliminary conclusions. The standard procedure for compensating ionospheric disturbances does not completely suppress disturbances associated with geomagnetic variations with periods from minutes to half an hour (geomagnetic pulsations and bays). A possible source of this phenomenon is modulation of the electron density in the ionosphere by charged particle fluxes, which, in turn, are modulated by the field of the MHD wave in the magnetosphere. This effect is height-differential, particle energy-dependent, resulting in «undercompensation» when using standard techniques for processing the apparent shift in the position of the base station. The effect does not occur for all geomagnetic pulsations of the same amplitude and frequency. To resolve the issue of practical significance of the detected effect and feasibility of further research, it is necessary to analyse variations in apparent displacement of the position of the object, determined by GNSS, taking into account the number of satellites and speed of the receiver, which is close to the real one.

New data on the thickness of the sedimentary cover and the structure of sedimentary basins in the most remote region of the continental Russian Arctic – the northeastern part of the Russian Federation – provide valuable information on the structure and conditions for formation of sedimentary rock strata in the region, including those promising for prospecting and exploration of mineral deposits. First of all, this is important for the search for hydrocarbon deposits on the shelf of the Arctic Ocean, as well as deposits of various mineral raw materials in the continental part of the Russian Arctic – coal deposits (Zyryansk basin), building materials, etc. The presented new models of the Moho section and the elastic parameters of the lithosphere also make it possible to refine data on the geological and tectonic structure of the territory and its development, including formation of mineral deposits in individual geological structures. The heat flow map compiled not only for the Russian Arctic, but for the entire circumpolar Arctic, is informative in terms of assessing the oil and gas content of the Russian Arctic and studying the thermal field of specific geomorphological structures associated with mantle degassing zones. Also, this map is useful for assessing the dynamics of water resources of ice sheets.

The obtained results of assessing the state of the lithosphere (both of the region as a whole and individual structures) are important geological and geophysical information that must be considered when designing and developing transport infrastructure in the Russian Arctic. Maps of the gravity field, the thickness of the sedimentary cover and the structure of sedimentary basins, and elastic parameters of the lithosphere provide comprehensive information about its geological structure, geodynamic conditions, and stress zones. These data are necessary for comprehensive assessment of suitability of the geological environment for design of railways, roads, airfields, and seaports, as well as pipelines and communication and power lines in the Russian Arctic. The heat flow map is informative in terms of assessing engineering-geological and environmental risks during construction and laying of highways in permafrost areas, as well as for predicting possible sea level changes due to glacier melting, which is important when designing seaports. The results obtained, both in combination and separately, are of high practical importance for development of the Russian Arctic region and its development.

The presented results on assessment of seismic hazard in the Russian Arctic are of strategic importance. The FCAZ-zones constructed for the eastern sector of the Russian Arctic define spatial regions within which the occurrence of epicenters of earthquakes with magnitude $M \geq 5{,}5$ is possible in the past, present, or future. In the identified zones marked in red-green colour (FCAZ-zones) in Pic. 20, special attention should be paid to safe operation of existing and yet planned new transport routes and facilities. These include the Northern Latitudinal Railway currently under construction in the Yamalo-Nenets Autonomous District. Increased attention in contoured areas should be paid to the seismic resistance of construction of new highways, sea and river ports, airports, railway infrastructures, etc. Special monitoring complexes should be created in the identified seismic zones that will provide reliable communication of the above transport infrastructure facilities with decision-making centres of the Ministry of Transport, Russian Railways, Aeroflot Russian Airlines, and the Ministry of Emergency Situations.

From the point of view of the seismological aspect of the studies performed, it should be noted the unprecedented importance of creating an integrated earthquake catalogue of the Russian Arctic, single in magnitude, implemented in the form of three independent information products: the integrated catalogue of the eastern part of the Russian Arctic, an integrated catalogue of the western part of the Russian Arctic, and an integrated catalogue of the Gakkel Ridge zone. The original method of integrating the catalogues of earthquakes of various agencies, which was created, can be considered as a significant advance in the part of seismology dedicated to the cataloguing of seismic events. The created method of system analysis is a significant contribution to development of geoinformatics.

Over the previous decades, the efforts of industrial organisations, research institutes and government agencies in Russia and abroad have accumulated significant arrays of spatial geological and geophysical information on the Arctic region. In recent years, this process has been significantly intensified with expansion of the observational network and the launch of specialised spacecraft, for example, the Arktika-M satellite [82]. Modern geoinformation systems allow efficient collection, storage, and intelligent analysis of spatial data in various disciplines in the field of earth sciences (e. g. [83; 84]).

To systematically analyse the impact of geophysical processes on the state and sustainable development of transport infrastructure in the Arctic, geoinformation methods and technologies for collecting, analysing, forecasting and presenting geological, geophysical and climatic data in the region are being developed. To create such a GIS, a client-server approach was chosen, implemented in the form of a thematic geoportal for user interaction with spatial information, a server part that operates the entire system, and a geodatabase that stores spatial information. In this model, the geodatabase combines information from various disciplines in geology, geophysics, and climatology.

In the course of studying the electromagnetic processes of the near-Earth environment and the effects of space weather on technological systems, data from a global high-precision model of the Earth's lithospheric magnetic field were included in the GIS database. Data on the lithospheric magnetic field are used in solving problems of navigation through the physical fields of the Earth. As part of the study of large geological structures and sedimentary basins, based on a comprehensive analysis of the gravity field and other geological and geophysical characteristics, data were collected on the detailed structure and properties of the Earth's lithosphere in the Russian Arctic region. The data collected in GIS reflect the complex dynamic processes taking place in the earth's crust, which must be considered in development of engineering infrastructure in the region. In the course of studies on assessment of seismic and other geodynamic hazards in the areas of promising development of the transport infrastructure of the Russian Arctic, the GIS included the most complete integrated catalogue of earthquakes necessary for spatial assessment of seismic activity.

When creating a GIS for the Russian Arctic, special attention is paid to the study of climatic processes that are critical for development of transport infrastructure in the region. Based on the data of long-term measurements of main climatic parameters (air temperature near the surface, soil temperature, total precipitation, wind speed near the earth's surface, soil moisture content, air humidity, snow cover thickness, change in the level of inland waters, etc.), relevant thematic maps and diagrams were built in GIS environment. Joint analysis of a wide range of climate data in a GIS environment makes it possible to assess the impact of current climate changes on transport infrastructure facilities (for example, permafrost thawing, increase in flood zones during seasonal floods). Thus, the formed database of spatial data, as well as a wide range of GIS tools for their analysis, is an important tool for assessing negative factors of the impact of various geophysical processes on the development of transport infrastructure in the Russian Arctic.

REFERENCES

1. Gvishiani, A. D., Rozenberg, I. N., Soloviev, A. A., Kostianoy, A. G., Gvozdik, S. A., Serykh, I. V., Krasnoperov, R. I., Sazonov, N. V., Dubchak, I. A., Popov, A. B., Kostianaia, E. A., Gvozdik, G. A. Electronic Atlas of Climatic Changes in the Western Russian Arctic in 1950–2021 as Geoinformatic Support of Railway Development. *Applied Sciences*, 2023, Vol. 13, Iss. 9, 5278. DOI: 10.3390/app13095278.

2. Johansson, J., Hassel, H., Cedergren, A. Vulnerability analysis of interdependent critical infrastructures: case study of the Swedish railway system. *International Journal of Critical Infrastructure*, 2011, Vol. 7, No. 4, pp. 289–316. DOI: https://doi.org/10.1504/IJCIS.2011.045065 [limited access].

3. Garmabaki, A. H. S., Marklund, S., Thaduri, A., Hedström, A., Kumar, U. Underground pipelines and railway infrastructure – failure consequences and restrictions. *Structure and Infrastructure Engineering. Maintenance, Management, Life-Cycle Design and Performance*, 2020, Vol. 16, Iss. 3, pp. 412–430. DOI: https://doi.org/10.1080/15732479.2019.1666885.

4. Oughton, E. J., Skelton, A., Horne, R. B., Thomson, A. W. P., Gaunt, C. T. Quantifying the daily economic impact of extreme space weather due to failure in electricity transmission infrastructure. *Space Weather*, 2017, Vol. 15, Iss. 1, pp. 65–83. DOI: https://doi.org/10.1002/2016SW001491.

5. Forte, B., Vani, B. C., Smith, N., Astin, I., Monico, J. F. G., Ruffenach, A., Flintoft, I., Concannon, A., McCormack, L., Koulouri, A. Space weather disruptions to satellite navigation and telecommunications in the case of interdependent services. 2018, poster session presented at 15th European Space Weather Week, Leuven, Belgium.

6. Gvishiani, A. D., Lukyanova, R. Yu., Soloviev, A. A. Geomagnetism: from the Earth's core to the Sun [*Geomagnetizm: ot yadra Zemli do Solntsa*]. Moscow, RAS publ., 2019, 186 p. ISBN: 978–5–907036–43–7.

7. Gvishiani A., Soloviev A. Observations, Modeling and Systems Analysis in Geomagnetic Data Interpretation. Springer International Publishing, 2020. DOI: 10.1007/978-3-030-58969-1 [limited access].

8. Pirjola, R., Kauristie, K., Lappalainen, H., Viljanen, A., Pulkkinen, A. Space weather risk. *Space Weather*, 2005, Vol. 3, Iss. 2. S02A02, DOI:10.1029/2004SW000112.

9. Pilipenko, V. A. Space weather impact on ground-based technological systems. *Solar-Terrestrial Physics*, 2021, Vol. 7, Iss. 3, pp. 73–110. DOI: https://doi.org/10.12737/szf-73202106.

10. Kasinskii, V. V., Ptitsyna, N. G., Lyahov, N. N., Tyasto, M. I., Villoresi, G., Iucci, N. Effect of geomagnetic disturbances on the operation of railroad automated mechanisms and telemechanics. *Geomagnetism and Aeronomy,* 2007, Vol. 47, Iss. 5, pp. 714–718. [Electronic resource]: https://www.elibrary.ru/item.asp?id=9534019. EDN: IAQLUJ. Last accessed 03.04.2023.

11. Eroshenko, E. A., Belov, A.V., Boteler, D., Gaidash, S. P., Lobkov, S. L., Pirjola, R., Trichtchenko, L. Effects of strong geomagnetic storms on Northern railways in Russia. *Advances in Space Research*, 2010, Vol. 46, Iss. 9, pp. 1102–1110. DOI: 10.1016/j.asr.2010.05.017.

12. Love, J. J., Hayakawa, H., & Cliver, E. W. Intensity and impact of the New York Railroad superstorm of May 1921. *Space Weather*, 2019, Vol. 17, Iss. 8, pp. 1281–1292. DOI: 10.1029/2019SW002250.

13. Silverman, S. M., Cliver, E. W. Low-latitude auroras: the magnetic storm of 14–15 May 1921. *Journal of Atmospheric and Solar-Terrestrial Physics*, 2001, Vol. 63, Iss. 5, pp. 523–535 DOI: https://doi.org/10.1016/S1364-6826(00)00174-7 [limited access].

14. Hapgood, M. The great storm of May 1921: An exemplar of a dangerous space weather event. *Space Weather*, Vol. 17, Iss. 7, pp. 950–975. DOI: 10.1029/2019SW002195

15. Wik, M., Pirjola, R., Lundstedt, H., Viljanen, A., Wintoft, P., Pulkkinen, A. Space weather events in July 1982 and October 2003 and the effects of geomagnetically induced currents on Swedish technical systems. *Annales Geophysica*e, 2009, Vol. 27, Iss. 4, pp. 1775–1787. DOI: https://doi.org/10.5194/angeo-27-1775-2009.

16. Pilipenko, V. A., Chernikov, A. A., Soloviev, A. A., Yagova, N. V., Sakharov, Ya. A., Kudin, D. V., Kostarev, D. V., Kozyreva, O. V., Vorobiev, A. V., Belov, A. V. Influence of Space Weather on the Reliability of the Transport System Functioning at High Latitudes. *Russian Journal of Earth Sciences*, 2023, Vol. 23, Iss. 2, pp. 1–34, ES2008. DOI: 10.2205/2023ES000824.

17. Ptitsyna, N. G., Tyasto, M. I., Kassinskii, V. V., Lyakhov, N. N., Villoresi, G. Do natural magnetic fields disturb railway telemetry? Proc. of 2007 7th International Symposium on Electromagnetic Compatibility and Electromagnetic Ecology, St. Petersburg, 26–29 June 2007, pp. 288–290. ISBN 9781424412693, IEEE # CFP07626-POD [limited access].

18. Ptitsyna, N. G., Kasinsky, V. V., Villoresi, G., Lyahov, N. N., Dorman, L. I., Iucci, N. Geomagnetic effects on mid-latitude railways: A statistical study of anomalies in the operation of signaling and train control equipment on the East-Siberian Railway. *Advances in Space Research*, 2008, Vol. 42, Iss. 9, pp. 1510–1514. DOI: https://doi.org/10.1016/j.asr.2007.10.015 [limited access].

19. Vorobev, A. V., Pilipenko, V. A., Sakharov, Ya. A., Selivanov, V. N. Statistical relationships between variations of the geomagnetic field, auroral electrojet and geomagnetically induced currents. *Solnechno-zemnaya fizika*, 2019, Vol. 5, Iss. 1, pp. 48–58. DOI: 10.12737/szf-51201905.

20. Vorobev, A., Soloviev, A., Pilipenko, V., Vorobeva, G., Sakharov, Y. An approach to diagnostics of geomagnetically induced currents based on ground magnetometers data. *Applied Sciences*, 2022, Vol. 12, Iss. 3, 1522. DOI: https://doi.org/10.3390/app12031522.

21. Sakharov, Ya. A., Yagova, N. V., Pilipenko, V. A. Pc5/pi3 geomagnetic pulsations and geomagnetically induced currents. *Bulletin of the Russian Academy of Sciences: Physics*, 2021, Vol. 85, Iss. 3, pp. 445–450. DOI: http://dx.doi.org/10.31857/s0367676521030236.

22. Yagova, N. V., Rozenberg, I. N., Gvishiani, A. D., Sakharov, Ya. A., Garanin, S. L., Voronin, V. A., Pilipenko, V. A., Dubchak, I. A. Study of the influence of geomagnetic activity on functioning of railway automation systems in the Arctic zone of Russia [*Issledovanie vliyaniya geomagnitnoi aktivnosti na funktsionirovanie sistem zheleznodorozhnoi avtomatiki v Arkticheskoi zone Rossii*]. *Arktika: ekologiya i ekonomika*, 2023, Vol. 13, Iss. 3 [в печати].

23. Chinkin, V. E., Soloviev, A. A., Pilipenko, V. A. Identification of vortex currents in the ionosphere and estimation of their parameters based on ground magnetic data. *Geomagnetism and Aeronomy*, 2020, Vol. 60, Iss. 5, pp. 588–599. DOI: 10.31857/S001679402005003X.

24. Chinkin, V. E., Soloviev, A. A., Pilipenko, V. A., Engebretson, M. J., Sakharov, Ya. A. Determination of vortex current structure in the high-latitude ionosphere with associated GIC bursts from ground magnetic data. *Journal of Atmospheric and Solar-Terrestrial Physics*, 2012, Vol. 212, 105514, DOI: https://doi.org/10.1016/j.jastp.2020.105514 [limited access; manuscript is accessible].

25. Newell, P. T., Liou, K., Zhang, Y., Sotirelis, T., Paxton, L. J., Mitchell, E. J. OVATION Prime-2013: Extension of auroral precipitation model to higher disturbance levels. *Space Weather*, 2014, Vol. 12, Iss. 6, pp. 368–379. DOI: 10.1002/2014SW001056.

26. Vorobev, A. V., Soloviev, A. A., Pilipenko, V. A., Vorobeva, G. R. Interactive computer model for aurora forecast and analysis. Solar-Terrestrial Physics, 2022, Vol. 8, Iss. 2, pp. 93–100. DOI: 10.12737/szf-82202213.

27. Vorobev, A. V., Soloviev, A. A., Pilipenko, V. A., Vorobeva, G. R. Internet Application for Interactive Visualization of Geophysical and Space Data: Approach, Architecture, Technologies. *Journal of the Earth and Space Physics*, 2023, Vol. 48, No. 4, pp. 151–160. DOI: 10.22059/jesphys.2023.350281.1007467.

28. Thaduri, A., Galar, D., Kumar, U. Railway assets: a potential domain for big data analytics. *Procedia Computer Science*, 2015, Vol. 53, pp. 457–467. DOI: https://doi.org/10.1016/j.procs.2015.07.323.

29. Kans, M., Galar, D., Thaduri, A. Maintenance 4.0 in Railway Transportation Industry. In: Koskinen, K., [*et al*]. Proceedings of the 10th World Congress on Engineering Asset Management (WCEAM 2015). *Lecture Notes in Mechanical Engineering*, 2016, Springer, Cham. DOI: https://doi.org/10.1007/978-3-319-27064-7_30 [limited access].

30. Jo, O., Kim, Y.-K., Kim, J. Internet of Things for Smart Railway: Feasibility and Applications. *IEEE Internet of Things Journal*, 2018, Vol. 5, No. 2, pp. 482–490. DOI: 10.1109/JIOT.2017.2749401.

31. Thaduri, A., Verma, A. K., Kumar, U. Maintenance of Railway Infrastructure Using Cyber-Physical Systems. In: Kapur, P. K., Singh, G., Klochkov, Y. S., Kumar, U. (eds). Decision Analytics Applications in Industry. Asset Analytics. Springer, Singapore, 2020, pp 521–540. DOI: https://doi.org/10.1007/978-981-15-3643-4_41 [limited access].

32. Pirjola, R. Effects of space weather on high-latitude ground systems. Advances in Space Research, 2005, Vol. 36, Iss. 12, pp. 2231–2240. DOI: https://doi.org/10.1016/j.asr.2003.04.074 [limited access].

33. Afraimovich, E. L., Perevalova, N. P. GPS-monitoring of the earth's upper atmosphere. Irkutsk, Institute of Solar-Terrestrial Physics SB RAS: GU NC RVH VSNC SO RAMN, 2006, 479 p. ISBN 5-98277-033-7.

34. Sato, H., Jakowski, N., Berdermann, J., Jiricka, K., Heßelbarth, A., Banyś, D., Wilken, V. Solar radio burst events on 6 September 2017 and its impact on GNSS signal frequencies. *Space Weather*, 2019, Vol. 17, Iss. 6, pp. 816–826. DOI: https://doi.org/10.1029/2019SW002198.

35. Cerruti, A. P., Kintner, P. M., Gary, D. E., Lanzerotti, L. J., de Paula, E. R., Vo, H. B. Observed solar radio burst effects on GPS/Wide Area Augmentation System carrier-to-noise ratio, *Space Weather*, 2006, Vol. 6, Iss. 4, S10006. DOI: https://doi.org/10.1029/2006SW000254.

36. Yasyukevich, Y. V., Yasyukevich, A. S., Astafyeva, E. I. How modernized and strengthened GPS signals enhance the system performance during solar radio bursts. *GPS Solutions*, 2021, Vol. 25, Iss. 2, art. 46. DOI: https://doi.org/10.1007/s10291-021-01091-5 [limited access].

37. Bisnath, S., Gao, Y. Precise Point Positioning – A Powerful Technique with a Promising Future. *GPS World*, April 2009, Iss. 4, pp. 43–50. [Electronic resource]: https://gge.ext.unb.ca/Resources/gpsworld.april09.pdf. Last accessed 03.04.2023.

38. Boteler, D. H., Pirjola, R. J., Nevanlinna, H. The effects of geomagnetic disturbances on electrical systems at the Earth's surface. *Advances in Space Research*, 1998, Vol. 22, Iss. 1, pp. 17–27. DOI: https://doi.org/10.1016/S0273-1177(97)01096-X [limited access].

39. Pirjola, R. Geomagnetically induced currents during magnetic storms. *IEEE Transactions on Plasma Science*, 2000, Vol. 28, Iss. 6, pp. 1867–1873. DOI: 10.1109/27.902215 [limited access].

40. Uspensky, M. I. Mitigating the impact of geomagnetic storms on the power system. *Izvestia Komi SC UB RAS*, 2017, Iss. 4 (32), pp. 116–122. [Electronic resource]: https://www.elibrary.ru/item.asp?id=32269413&ysclid=lktqioxq3h876970014. Last accessed 03.04.2023.

41. Gaunt, C. T. Why space weather is relevant to electrical power systems. *Space Weather*, 2016, Vol. 14, Iss. 1, pp. 2–9. DOI: https://doi.org/10.1002/2015SW001306.

42. Krausmann, E., Andersson, E., Russell, T., Murtagh, W. Space Weather and Rail: Findings and Outlook (European Commission, JRC Science and Policy Reports), 2015. DOI: 10.2788/211456.

43. Apatenkov, S. V., Pilipenko, V. A., Gordeev, E. I., Viljanen, A., Juusola, L., Belakhovsky, V. B., Sakharov, Ya. A., Selivanov, V. N. Auroral omega bands are a significant cause of large geomagnetically induced currents. *Geophysical Research Letters*, 2020, Vol. 47, Iss. 6, e2019GL086677. DOI: https://doi.org/10. 1029/2019GL086677.

44. Yagova, N. V., Pilipenko, V. A., Sakharov, Ya. A., Selivanov, V. N. Spatial scale of geomagnetic Pc5/Pi3 pulsations as a factor of their efficiency in generation of geomagnetically induced currents. *Earth, Planets and Space*, 2021, Vol. 73, art. 88. DOI: https://doi.org/10.1186/s40623-021-01407-2.

45. Sakharov, Ya. A., Yagova, N. V., Pilipenko, V. A., Selivanov, V. N. Spectral content of pc5–6/pi3 geomagnetic pulsations and their efficiency in generation of geomagnetically induced currents. *Russian Journal of Earth Sciences*, 2022, Vol. 22, Iss. 1, pp. 1–9. DOI: http://dx.doi.org/10.2205/2021es000785.

46. Matandirotya, E., Cilliers, P. J., Van Zyl, R. R., Oyedokun, D. T., de Villiers, J. Differential magnetometer method applied to measurement of geomagnetically induced currents in Southern African power networks. *Space Weather*, 2016, Vol. 14, Iss. 3, pp. 221–232. DOI: https://doi.org/10.1002/2015SW001289.

47. Hübert, J., Beggan, C. D., Richardson, G. S., Martyn, T., Thomson, A. W. P. Differential magnetometer measurements of geomagnetically induced currents in a complex high voltage network. *Space Weathe*r, 2020, Vol. 18, Iss. 4, e2019SW002421. DOI: https://doi.org/10.1029/2019SW002421.

48. Torta, J. M., Marsal, S., Ledo, J., Queralt, P., Canillas-Pérez, V., Piña-Varas, P., Curto, J. J., Marcuello, A., Martí, A. New detailed modeling of GICs in the Spanish power transmission grid. *Space Weather*, 2012. Vol. 19, Iss. 9, e2021SW002805. DOI: https://doi.org/10.1029/2021SW002805.

49. Watari, S., Nakamura, S., Ebihara, Y. Measurement of geomagnetically induced current (GIC) around Tokyo, Japan. *Earth, Planets and Space*, 2021, Vol. 73, 102. DOI: https://doi.org/10.1186/s40623-021-01422-3.

50. Alves Ribeiro, J., Pinheiro, F. J. G., Pais, M. A., Santos, R., Cardoso, J., Baltazar-Soares, P., & Monteiro Santos, F. A. Toward More Accurate GIC Estimations in the Portuguese Power Network. *Space Weather*, 2023, Vol. 21, Iss. 6, e2022SW003397. DOI: https://doi.org/10.1029/2022SW003397.

51. Landau, L. D., Lifshits, E. M. Field theory [Teoriya polya]. 7th ed., rev. Moscow, Nauka publ., 1988, 512 p. («Theoretical physics», Vol. II). ISBN 5-02-014420-7.

52. Soloviev, A., Dobrovolsky, M., Kudin, D., Sidorov, R. Minute values of X, Y, Z components and total intensity F of the Earth's magnetic field from Geomagnetic Observatory Klimovskaya (IAGA code: KLI). ESDB repository. Geophysical Center of the Russian Academy of Sciences. 2015. DOI: 10.2205/kli2011min.

53. Soloviev, A. A., Sidorov, R. V., Krasnoperov, R. I., Grudnev, A. A. Khokhlov, A. V. Klimovskaya: a new geomagnetic observatory. *Geomagnetism and Aeronomy*, 2016, Vol. 56, Iss. 3, pp. 365–379. DOI: 10.7868/S0016794016030160.

54. Kaban, M. K., Sidorov, R. V., Soloviev, A. A., Gvishiani, A. D., Petrunin, A. G., Petrov, O. V., Kashubin, S. N., Androsov, E. A., Milshtein, E. D. A New Moho Map for North-Eastern Eurasia Based on the Analysis of Various Geophysical Data. *Pure and Applied Geophysics*, 2022, Vol. 179, Iss. 11, pp. 3903–3916. DOI: https://doi.org/10.1007/s00024-021-02925-6.

55. Petrov, O., Morozov, A., Shokalsky, S., Kashubin, S., Artemieva, I. M., Sobolev, N., Petrov, E., Ernst, R. E., Sergeev, S., Smelror, M. Crustal structure and tectonic model of the Arctic region. *Earth-Science Reviews*, 2016, Vol. 154, March, pp. 29–71. DOI: https://doi.org/10.1016/j.earscirev.2015.11.013.

56. Sidorov, R. V., Kaban, M. K., Soloviev, A. A., Petrunin, A. G., Gvishiani, A. D., Oshchenko, A. A., Popov, A. B., Krasnoperov, R. I. Sedimentary basins of the eastern Asia Arctic zone: new details on their structure revealed by decompensative gravity anomalies. *Solid Earth*, 2021, Vol. 12, Iss. 12, pp. 2773–2788. DOI: https://doi.org/10.5194/se-12-2773-2021.

57. Petrunin, A. G., Soloviev, A. A., Sidorov, R. V., Gvishiani, A. D. Inverse-forward method for heat flow estimation: case study for the Arctic region. *Russian Journal of Earth Sciences*, 2023, Vol. 22, № 6, pp. 1–9. DOI: https://doi.org/10.2205/2022ES000809.

58. Davies, J. H. Global map of solid Earth surface heat flow. *Geochemistry, Geophysics, Geosystems*, 2013, Vol. 14, Iss. 10, pp. 4608–4622. DOI: https://doi.org/10.1002/ggge.20271.

59. Lucazeau, F. Analysis and mapping of an updated terrestrial heat flow data set. *Geochemistry, Geophysics, Geosystems*, 2019, Vol. 20, Iss. 8, pp. 4001–4024. DOI: https://doi.org/10.1029/2019GC008389.

60. Kaban, M. K., Chen, B., Tesauro, M., Petrunin, A. G., El Khrepy, S., Al-Arifi, N. Reconsidering Effective Elastic Thickness Estimates by Incorporating the Effect of Sediments: A Case Study for Europe. *Geophysical Research Letters*, 2018, Vol. 45, Iss. 18, pp. 9523–9532. DOI: https://doi.org/10.1029/2018GL079732.

61. Soloviev, A., Petrunin, A., Gvozdik, S., Sidorov, R. A Set of Geophysical Fields for Modeling of the Lithosphere Structure and Dynamics in the Russian Arctic Zone. *Data*, 2023, Vol. 8, Iss. 5, 91. DOI: https://doi.org/10.3390/data8050091.

62. Shebalin, P. N., Gvishiani, A. D., Dzeboev, B. A., Skorkina, A. A. Why are new approaches to seismic hazard

assessment required? *RAS reports. Earth Sciences*, 2022, Vol. 507, Iss. 1, pp. 91–97. DOI: 10.31857/S2686739722601466.

63. Ulomov, V. I., The GSHAP Region 7 Working Group. Seismic hazard of Northern Eurasia. *Annali di Geofisica*, 1999, Vol. 42, No. 6, pp. 1023–1038. DOI: https://doi.org/10.4401/ag-3785.

64. Zaliapin, I., Ben-Zion, Y. Earthquake clusters in southern California. I: Identification and stability. *Journal of Geophysical Research: Solid Earth*, 2013, Vol. 118, Iss. 6, pp. 2847–2864. DOI: https://doi.org/10.1002/jgrb.50179.

65. Zaliapin, I., Ben-Zion, Y. A global classification and characterization of earthquake clusters. *Geophysical Journal International*, 2016, Vol. 207, Iss. 1, pp. 608–634. DOI: https://doi.org/10.1093/gji/ggw300.

66. Vorobieva, I. A., Gvishiani, A. D., Dzeboev, B. A., Dzeranov, B. V., Barykina, Y. V., Antipova, A. O. Nearest Neighbor Method for Discriminating Aftershocks and Duplicates When Merging Earthquake Catalogs. *Frontiers in Earth Science*, 2022, Vol. 10, 820277. DOI: 10.3389/feart.2022.820277.

67. Gvishiani, A. D., Vorobieva, I. A., Shebalin, P. N., Dzeboev, B. A., Dzeranov, B. V., Skorkina, A. A. Integrated Earthquake Catalog of the Eastern Sector of the Russian Arctic. *Applied Sciences*, 2022, Vol. 12, Iss. 10, 5010. DOI: https://doi.org/10.3390/app12105010.

68. Vorobieva, I. A., Gvishiani, A. D., Shebalin, P. N., Dzeboev, B. A., Dzeranov, B. V., Skorkina, A. A., Sergeeva, N. A., Fomenko, N. A. Integrated Earthquake Catalog II: The Western Sector of the Russian Arctic. *Applied Sciences,* 2023, Vol. 12, Iss. 12, 7084. DOI: https://doi.org/10.3390/app13127084.

69. Gvishiani, A. D., Dzeboev, B. A., Dzeranov, B. V., Kedrov, E. O., Skorkina, A. A., Nikitina, I. M. Strong Earthquake-Prone Areas in the Eastern Sector of the Arctic Zone of the Russian Federation. *Applied Sciences*, 2022, Vol. 12, Iss. 23, 11990. DOI: https://doi.org/10.3390/app122311990.

70. Shebalin, P. N., Narteau, C., Baranov, S. V. Earthquake productivity law. *Geophysical Journal International*, 2020, Vol. 222, Iss. 2, pp. 1264–1269. DOI: https://doi.org/10.1093/gji/ggaa252.

71. Gvishiani, A. D., Dzeboev, B. A., Agayan, S. M. FCaZm intelligent recognition system for locating areas prone to strong earthquakes in the Andean and Caucasian mountain belts. *Physics of Solid Earth*, 2016, Iss. 4, pp. 3–23. DOI: 10.7868/S0002333716040013.

72. Ogata, Y. Statistical model for standard seismicity and detection of anomalies by residual analysis. *Tectonophysics*, 1989, Vol. 169, Iss. 1–3, pp. 159–174. DOI: https://doi.org/10.1016/0040-1951(89)90191-1.

73. Zhuang, J., Ogata, Y., Vere-Jones, D. Analyzing earthquake clustering features by using stochastic reconstruction. *Journal of Geophysical Research: Solid Earth*, 2004, Vol. 109, Iss. B5, B05301. DOI: https://doi.org/10.1029/2003JB002879.

74. Baranov, S. V., Gvishiani, A. D., Narteau, C., Shebalin, P. N. Epidemic type aftershock sequence exponential productivity. *Russian Journal of Earth Sciences*, 2019, Vol. 19, Iss. 6, ES6003. DOI: 10.2205/2019ES000695.

75. Dzeboev, B. A., Gvishiani, A. D., Agayan, S. M., Belov, I. O., Karapetyan, J. K., Dzeranov, B. V., Barykina, Y. V. System-Analytical Method of Earthquake-Prone Areas Recognition. *Applied Sciences*, 2021, Vol. 11, Iss. 17, 7972. DOI: https://doi.org/10.3390/app11177972.

76. Thébault, E., Hulot, G., Langlais, B., Vigneron, P. A Spherical Harmonic Model of Earth's Lithospheric Magnetic Field up to Degree 1050. *Geophysical Research Letters*, 2021, Vol. 48, Iss. 21, e2021GL095147. DOI: https://doi.org/10.1029/2021GL095147.

77. Soloviev, A. A., Sidorov, R. V., Oshchenko, A. A., Zaitsev, A. N. On the Need for Accurate Monitoring of the Geomagnetic Field during Directional Drilling in the Russian Arctic. *Izvestiya, Physics of the Solid Earth,* 2022, Iss. 3, pp. 136–152. DOI:10.31857/S0002333722020120.

78. Vorobiev, A. V., Soloviev, A. A., Pilipenko, V. A., Vorobieva, G. R., Gainetdinova, A. A., Lapin, A. N., Belakhovsky, V. B., Roldugin, A. V. Diagnostics of aurora presence based on intelligent analysis of geomagnetic data, *Solnechno-zemnaya fizika,* 2023, Vol. 9, Iss. 2, pp. 26–34. DOI: https://doi.org/10.12737/szf-92202303.

79. Rozenberg, I. N., Gvishiani, A. D., Soloviev, A. A., Voronin, V. A., Pilipenko, V. A. Influence of space weather on reliability of railway transport in the Arctic zone of Russia [*Vliyanie kosmicheskoi pogody na nadezhnost funktsionirovaniya zheleznodorozhnogo transporta v Arkticheskoi zone Rossii*]. *Zheleznodorozhniy transport*, 2021, Iss. 12, pp. 20–26. [Electronic resource]: https://www.elibrary.ru/item.asp?edn=zhbcew&ysclid=lktpuha4xl415913232 [limited access].

80. Petrukovich, A. A., Breus, T. K., Deminov, M. G., Dmitriev, A. V., Krivolutsky, A. A., Petrov, V. M., Pulinets, S. A., Raspopov, O. M., Nagovitsyn, Yu. A., Trishchenko, L. D., Troshichev, O. A. Space weather effects. Geomagnetic disturbances and power supply and wire communication systems. In the book: Plasma heliogeophysics. Monograph: in 2 Vol. [M. A. Livshits et al]; ed. by L. M. Zeleny and I. S. Veselovsky. Moscow, Fizmatlit publ., 2008, Vol. 2, 559 p., pp. 213–219. ISBN 978-5-9221-1041-9.

81. Liu, L., Ge, X., Zong, W., Zhou, Y., Liu, M. Analysis of the monitoring data of geomagnetic storm interference in the electrification system of a high-speed railway. *Space Weather*, 2016, Vol. 14, Iss. 10, pp. 754–763. DOI: https://doi.org/10.1002/2016SW001411.

82. Asmus, V. V., Milekhin, O. E., Kramareva, L. S., Khailov, M. N., Shirshakov, A. E., Shumakov, I. A. The world's first highly elliptical hydrometeorological space system Arktika-M [*Pervaya v mire vysokoellipticheskaya gidrometeorologicheskaya kosmicheskaya Sistema «Arktika-M»*]. *Meteorology and Hydrology*, 2021, Iss. 12, pp. 11–26. DOI 10.52002/0130–2906–2021–12–11–26.

83. Soloviev, A., Khokhlov, A., Jalkovsky, E., Berezko, A., Lebedev, A., Kharin, E., Shestopalov, I., Mandea, M., Kuznetsov, V., Bondar, T., Mabie, J., Nisilevich, M., Nechitailenko, V., Rybkina, A., Pyatygina, O., Shibaeva, A. The Atlas of the Earth's Magnetic Field. (Eds.: Gvishiani, A., Frolov, A., Lapshin, V.). Publ. GC RAS, Moscow, 2013, 361 p. ISBN 978-5-904509-13-2. DOI: 10.2205/2013BS011_Atlas_MPZ.

84. Soloviev, A. A., Soloviev, A. A., Gvishiani, A. D., Nikolov, B. P., Nikolova, Y. I. GIS-oriented database on seismic hazard assessment for Caucasian and Crimean regions. *Issledovanie Zemli iz kosmosa*, 2018, Iss. 5, pp. 52–64. DOI: 10.31857/S020596140003241-6. ●

Information about the authors:

Gvishiani, Alexey D., *D.Sc. (Physics and Mathematics), Professor, Academician of the Russian Academy of Sciences, Chairman of the Academic Council of Geophysical Centre of the Russian Academy of Sciences, Moscow, Russia.*

Rozenberg, Igor N., *D.Sc. (Eng), Professor, Corresponding Member of the Russian Academy of Sciences, Vice-rector of Russian University of Transport; JSC NIIAS, Moscow, Russia, i.rozenberg@geosc.ru.*

Soloviev, Anatoly A., *D.Sc. (Physics and Mathematics), Corresponding Member of the Russian Academy of Sciences, Professor of the Russian Academy of Sciences, director of Geophysical Centre of the Russian Academy of Sciences, Moscow, Russia.*

Article received 04.11.2022, approved 17.02.2023, updated 26.06.2023, accepted 28.06.2023.